

CONTENTS

Fast and furious: Astronomers reveal best image yet of mysterious ORCs in space24
In the wake of a dying Sun26
Megamaser “Nkalakatha” discovered by astronomers using MeerKAT29
Observations and images of Comet C/2021 A1 (Leonard)32
Streicher Asterisms57
Webinars62



In this issue:

News Notes – Odd Radio Circles (ORCS)

Wake structures around stars

MeerKAT Megamaser

Comet C/2021 A1 (Leonard)

Webinars

Streicher Asterisms

EDITORIAL BOARD	Mr Case Rijdsijk (Editor, <i>MNASSA</i>) Mr Auke Slotegraaf (Editor, <i>Sky Guide Africa South</i>) Mr John Gill (Webmaster) Mr James Smith (Web Manager) Dr I.S. Glass (Member, S A Astronomical Observatory) Dr V. McBride (Member, OAD-IAU) Mr Maciej Soltynski (Book Review Editor) Prof B. Warner (Member, University of Cape Town)
MNASSA PRODUCTION	Mr Case Rijdsijk (Editor, <i>MNASSA</i>) Dr Ian Glass (Assistant Editor) Mr Willie Koorts (Publication on Web)
EDITORIAL ADDRESSES	MNASSA, PO Box 9, Observatory 7935, South Africa Email: mnassa@sao.ac.za Web Manager: smi.james.th@gmail.com MNASSA Download Page: www.mnassa.org.za
SUBSCRIPTIONS	<i>MNASSA</i> is available for free on the Internet
ADVERTISING	Advertisements may be placed in <i>MNASSA</i> at the following rates per insertion: full page R400, half page R200, quarter page R100. Small advertisements R2 per word. Enquiries should be sent to the editor at mnassa@sao.ac.za
CONTRIBUTIONS	<i>MNASSA</i> mainly serves the Southern African astronomical community. Articles may be submitted by members of this community or by those with strong connections. Else they should deal with matters of direct interest to the community. <i>MNASSA</i> is published on the first day of every second month and articles are due one month before the publication date.
RECOGNITION	Articles from <i>MNASSA</i> appear in the NASA/ADS data system.

Cover: Comet Leonard image on December 24, 2021, by Tiaan Niemand. See article on page 32.

The **Astronomical Society of Southern Africa** (ASSA) was formed in 1922 by the amalgamation of the Cape Astronomical Association (founded 1912) and the Johannesburg Astronomical Association (founded 1918). It is a body consisting of both amateur and professional astronomers.

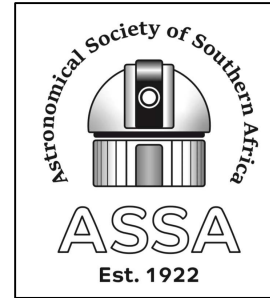
Publications: The Society publishes its electronic journal, the *Monthly Notes of the Astronomical Society of Southern Africa (MNASSA)* bi-monthly, the annual *Sky Guide Africa South* and *Nightfall*.

Membership: Membership of the Society is open to all. Potential members should consult the Society's web page : <http://assa.sao.ac.za> for details. Joining is possible via one of the local Centres or as a Country Member.

Local Centres: Local Centres of the Society exist at Bloemfontein, Cape Town, Durban, Hermanus, Johannesburg, Pretoria and the Garden Route Centre; membership of any of these Centres automatically confers membership of the Society.

Internet contact details: email: assa@sao.ac.za Home Page: <http://assa.sao.ac.za>

ASSA Council	
President	Chris Stewart
Vice-President (outgoing)	Case Rijdsijk
Vice President (Incoming)	Dr Daniel Cunnama
Membership Secretary	Eddie Nijeboer
Treasurer	AJ Nel
Secretary	Lerika Cross
Council Member	Dr Pierre de Villiers
Council Member	Dr Ian Glass
Bloemfontein Chair	Thinus van der Merwe
Cape Chair	Christian Hettlage (AC)
Durban Chair	Amith Rajpal
Garden Route Chair	Case Rijdsijk
Hermanus Chair	Dr Pierre de Villiers
Johannesburg Chair	Allison Coulter
Pretoria Chair	Bosman Olivier
Council Appointees	
Scholarships	Claire Flanagan
ASSA Communication Coordinator	Dr Sally MacFarlane
Webmaster	John Gil
Section Directors	
Dark Sky	Dr Daniel Cunnama
Observing section	Angus Burns
Photometry, Spectroscopy	Percy Jacobs
Cosmology/Astrophysics	Bruce Dickson
History	Chris de Coning
Double and Variable Stars	Dave Blane
Imaging	Martin Heigan
Instrumentation and ATM	Chris Stewart
Citizen Science	Allen Versfeld
Comet, Asteroid and Meteor Section	Tim Cooper



Fast and furious: Astronomers reveal best image yet of mysterious ORCs in space

Astronomy's newest mystery objects, odd radio circles or ORCs, have been pulled into sharp focus by an international team of astronomers using the world's most capable radio telescopes.

First revealed by the ASKAP radio telescope, owned and operated by Australia's national science agency CSIRO, odd radio circles quickly became objects of fascination. Theories on what caused them ranged from galactic shockwaves to the throats of wormholes.

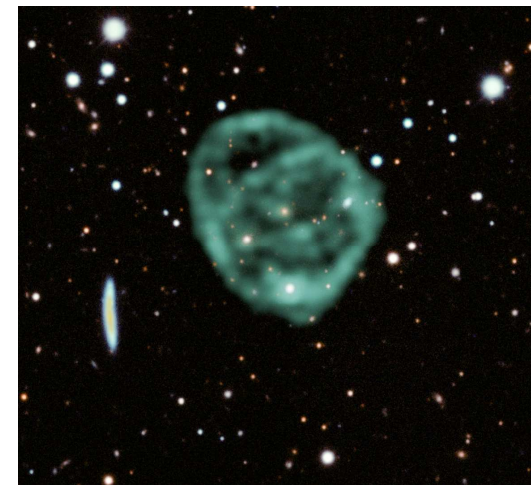


Fig. 1 *The MeerKAT Stokes-I image of ORC1, superimposed on optical data from the Dark Energy Survey DR1 (Abbott et al. 2018), both spanning the same field of view. A square root transfer function was applied to the radio data of the field of view and this grayscale image was then adjusted for contrast. An image of the radio data confined to the ORC region was assigned mint green. This region was blended with the greyscale radio continuum field of view image and the DES optical image of the same field, so*

that faint radio sources outside the ORC appear as faint grey diffuse patches, often surrounding their host galaxies. The filters used in the DES image were assigned turquoise, magenta, yellow and red, with the result that DES sources mainly appear in this image as white. The layering schema employed is described in English (2017). This figure is optimised to convey the structure of the ORC, and quantitative information should be taken from Figure 1 or from the FITS files in the Supplementary Information.

A new detailed image, captured by the South African Radio Astronomy Observatory's MeerKAT radio telescope and published today in Monthly Notices of the Royal Astronomical Society (DOI 10.1093/mnras/stac701), is providing researchers with more information to help narrow down those theories.

To date ORCs have only been detected using radio telescopes, with no signs of them when researchers have looked for them using optical, infrared, or X-ray telescopes.

Dr Jordan Collier of the Inter-University Institute for Data Intensive Astronomy, who compiled the image from MeerKAT data said continuing to observe these odd radio circles will provide researchers with more clues.

People often want to explain their observations and show that it aligns with our best knowledge. To me, it's much more exciting to discover something new, that defies our current understanding, said Dr Collier.

The rings are enormous – about a million light years across, which is 16 times bigger than our own galaxy. Despite this, odd radio circles are hard to see.

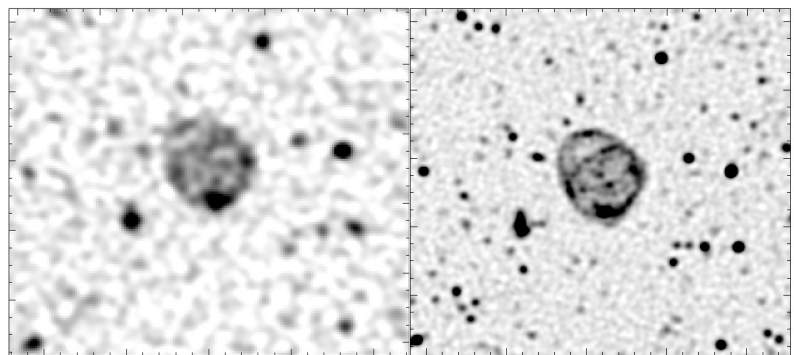


Fig. 2 ASKAP and MeerKAT: (Left) The ASKAP image of ORC1, adapted from Norris et al. (2021b) at 944 MHz. The resolution is 11 arcsec, and the rms sensitivity is 25 μ Jy/beam. (Right) The new Meerkat image of ORC1 at 1284 MHz. The resolution is 6 arcsec, and the rms sensitivity is 2.4 μ Jy/beam.

resolution is 6 arcsec, and the rms sensitivity is 2.4 μ Jy/beam.

Professor Ray Norris from Western Sydney University and CSIRO, one of the authors on the paper, said only five odd radio circles have ever been revealed in space.

We know ORCs are rings of faint radio emissions surrounding a galaxy with a highly active black hole at its centre, but we don't yet know what causes them, or why they are so rare, he continued.

Dr Fernando Camilo, Chief Scientist of the South African Radio Astronomy Observatory, which built and operates MeerKAT, said that the ORC project is a great example of the clever use of MeerKAT by its users, playing to its strengths: ASKAP observes large swaths of the sky and can discover relatively rare types of objects; MeerKAT can then follow up to study them in greater detail.

This presentation will discuss DH in general and provide a brief overview of the situation of DH in South Africa. Next, the South African Centre for Digital Language Resources (SADiLaR) will be introduced including some of the activities SADiLaR organizes. Next, show some more general computational techniques applied to humanities data. These examples will hopefully lead to new ideas of combining computational techniques (which may stem from the field of astronomy) and humanities data.

To really understand ORCs scientists will need access to even more sensitive radio telescopes such as those of the SKA Observatory, which is supported by more than a dozen countries including South Africa, Australia, the UK, France, Canada, China and India.

Prof. Norris was confident that once the SKA telescopes, were built, many more ORCs will be found and will be able to tell us more about the lifecycle of galaxies.

But until the SKA becomes operational, ASKAP and MeerKAT are set to revolutionise our understanding of the Universe faster than ever before.

In the wake of a dying Sun

A team of scientists from the South African Astronomical Observatory (SAAO), Michigan State University (MSU), and the University of Miami (UM) have created novel 3D simulations to investigate how dying stars interact with their environment and nearby planets. The team created simulations of the interaction of red giant stars which eject dense outflows of gas and dust into their surroundings, on nearby companions such as planets and brown dwarfs. In this way, they are able to study the effect of such close companions on the stellar outflow properties (e.g., its shape, mass and momentum).

These simulations show that the interaction of the nearby companion with the stellar winds or outflows creates complex structures, such as spirals, arcs and bars, said Dr Elias Aydi, a Research Associate at MSU and a former PhD student at SAAO, who led the study along with Prof Shazrene Mohamed (UM and SAAO). The simulations give us a peek into what the solar system might look like when our Sun turns into a giant star, in a few billion years from now.

At the end of their lifetimes, stars like our Sun become unstable and expand in size, turning into red giants. During this phase, the extended outer layers are only loosely bound to the star by gravity, so the star loses a considerable amount of its mass through stellar winds. Our Sun is expected to turn into a giant star in a few billion years from now, likely expanding beyond Earth's orbit, and swallowing the inner planets like Mercury, Venus, and our Earth.

At a certain point of the giant phase, a star with a mass close to that of the Sun experiences regular pulsations with periods longer than 100 days. These pulsations are actual expansion and contraction of the unstable atmosphere of the giant star, in an attempt for the star to regain its equilibrium. The brightness of the star oscillates due to the pulsations, showing an increase by a factor of 10 up to more than 100. The

pulsations produce radial shock waves that travel through the circumstellar environment, similar to ripples propagating on the surface of a pond when we throw a rock into it.

According to Prof Mohammed these shock-waves interact with the wake of the nearby companion producing even stronger, enhanced shocks --- regions of abrupt change in velocity, temperature, and density. The process is similar to what happens when ocean waves meet the wake of a speedboat, just more extreme.

While the companion orbits the giant star, it periodically meets a new cycle of stellar pulsations. If there is a certain resonance between the orbital period of the companion and the stellar pulsations, i.e., the companion meets the stellar pulsations every time around the same place, the strong shocks between the pulsations and the companion wakes cluster into multiple spiral structures, extending for billions of kilometres around the system.

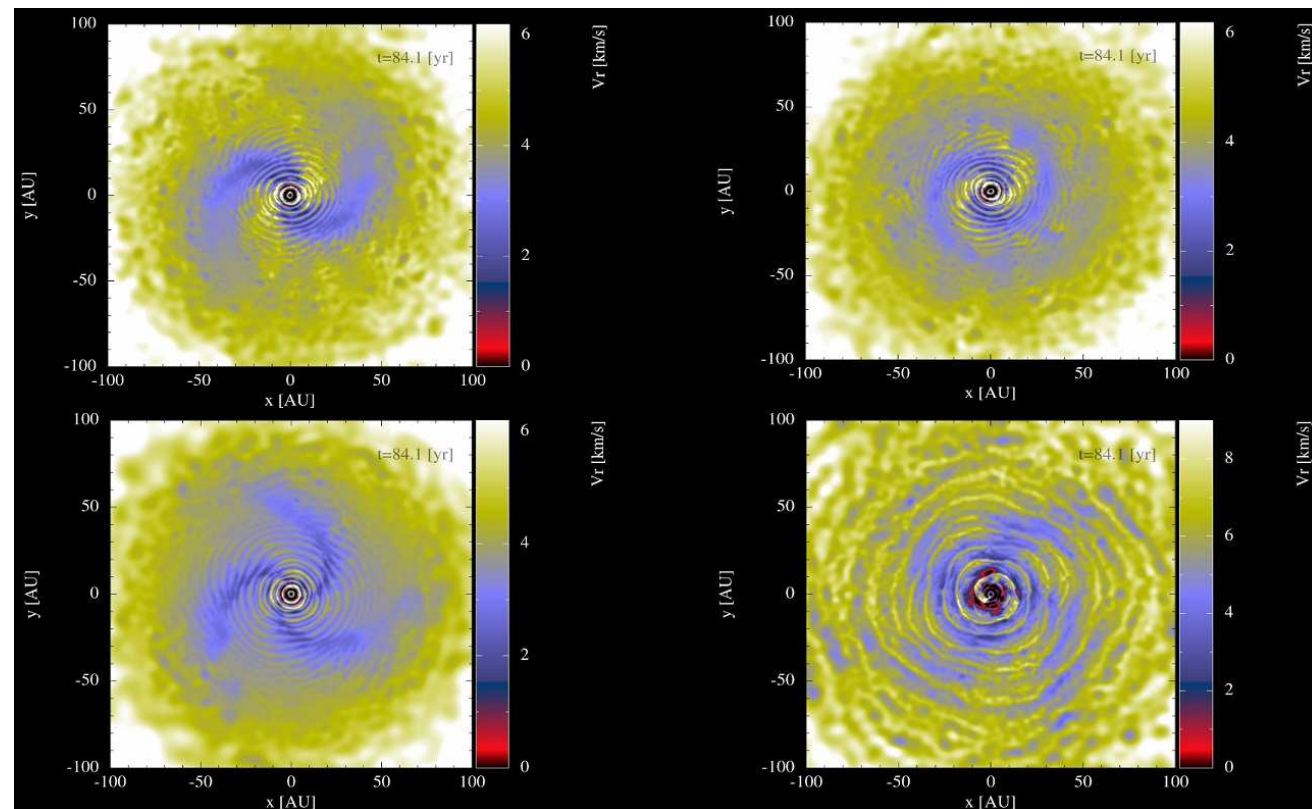


Fig 1: These images show four different possible patterns that could emerge around a giant star, orbited by a nearby giant planet. Each image shows a broad expanse of space — billions of miles across — with the star as a black orb at the centre. The companion is too small to see clearly at this scale, but it creates a visible wake behind it as it travels through the gas and dust that fill the circumstellar environment. The gas is coloured shades of green and blue, with green gas moving faster than blue. It's in the green gas that we see different possible patterns: two-armed, three-armed, and four-armed spirals. Credit: Elias Aydi/MSU

misspecification in Bayesian deep-learning. I will go on to talk about how the effect of data curation can also affect the use of semi-supervised learning that leverages large unlabelled datasets - highly relevant for radio astronomy applications where the volume of labelled catalogue data is small, but the quantity of archival survey data is large.

Title: Gas Stripping and Star Formation in Galaxy Clusters

Speaker: Dr Mpati Ramatsoku from Rhodes University.

Date: 1 April

Venue: UKZN Zoom

Time: 15h00 SAST

Abstract: It is now well established that the star formation activity in galaxies has strongly declined since $z \sim 2$. To identify the cause of the decline of star formation (SF) and the emergence of the different galaxy types, it is crucial to understand the processes of gas acquisition and loss. Gas is the fuel for SF and a sensitive tracer of both the environmental effects and internal feedback. Galaxies falling into high-density environments such as clusters experience gas removal due to the interaction with the intra-cluster medium, i.e., ram pressure stripping. An extreme example of rapid galaxy transformation due to this phenomenon is seen in galaxies that exhibit long tails of stripped gas/debris material.

The removal of gas as it occurs in these galaxies can be studied in various ways, but one of the primary methods is to examine their HI gas content.

In this talk, I will discuss the correlation between the HI gas content and star formation efficiencies of these long-tailed galaxies in relation to the impact of the ram pressure stripping events.

Title: Digital Humanities and potential links to Astronomy

Speaker: Prof Menno van Zaanen, Professor in Digital Humanities North West University Potchefstroom, South African Centre for Digital Language Resources.

Date: 21 April

Venue: SAAO - Zoom

Time: 11h00 SAST

Abstract: Digital humanities (DH) is a relatively new research area (in particular in South Africa), which sits on the boundary between the fields of humanities and computing. On the one hand, incorporating computational techniques to the field of humanities allows, for example for the handling of large amounts of data, whereas, on the other hand, the field of humanities provides interesting data sets that can be used to develop and test computational techniques.

TIFR/NCRA building an ultra-wide field of view telescope for identifying and localising the brightest and rarest FRBs and possible prompt EM counterparts of BNS mergers..

Title: Resolving the formation and evolution of primeval galaxies: from re-ionisation to cosmic noon

Speaker: Dr David Sobral from Lancaster University - University of Lisbon

Date: 11 March

Venue: UWC Zoom

Time: 11h30

Abstract: I will present new results that reveal the nature and evolution of primeval galaxies, picked up in large and deep surveys due to their Lyman-alpha emission. I will show how Lyman-alpha emitters (LAEs) are an incredibly rare population of galaxies in the local Universe, but become dominant into the epoch of re-ionisation and that they have the properties and the number density necessary to dominate and drive cosmic re-ionisation.

Lyman- α ($\text{Ly}\alpha$) is intrinsically the brightest line emitted from active galaxies, but its resonant nature and susceptibility to dust as a rest-frame UV photon makes $\text{Ly}\alpha$ very hard to interpret due to the uncertain $\text{Ly}\alpha$ escape fraction, until now. By conducting large blind surveys at different cosmic times and the necessary spectroscopic follow-up, we have obtained a simple empirical relation that robustly retrieves the $\text{Ly}\alpha$ escape fraction as a function of $\text{Ly}\alpha$ rest-frame EW. We show that the relation constrains a well-defined anti-correlation between ionisation efficiency and dust extinction in Lyman-alpha emitters (LAEs) which is likely an evolutionary sequence for very young metal poor sources going through a LAE phase. We also reveal how those LAEs/primeval galaxies have high escape fractions of not just Lyman-alpha photons, but also LyC , and how the production and escape seem to be linked together.

Title: Catalogue curation, likelihood misspecification & dataset shift: challenges for Bayesian deep-learning in radio astronomy

Speaker: Dr Anna Scaife from Jodrell Bank Centre for Astrophysics

Date: 18 March

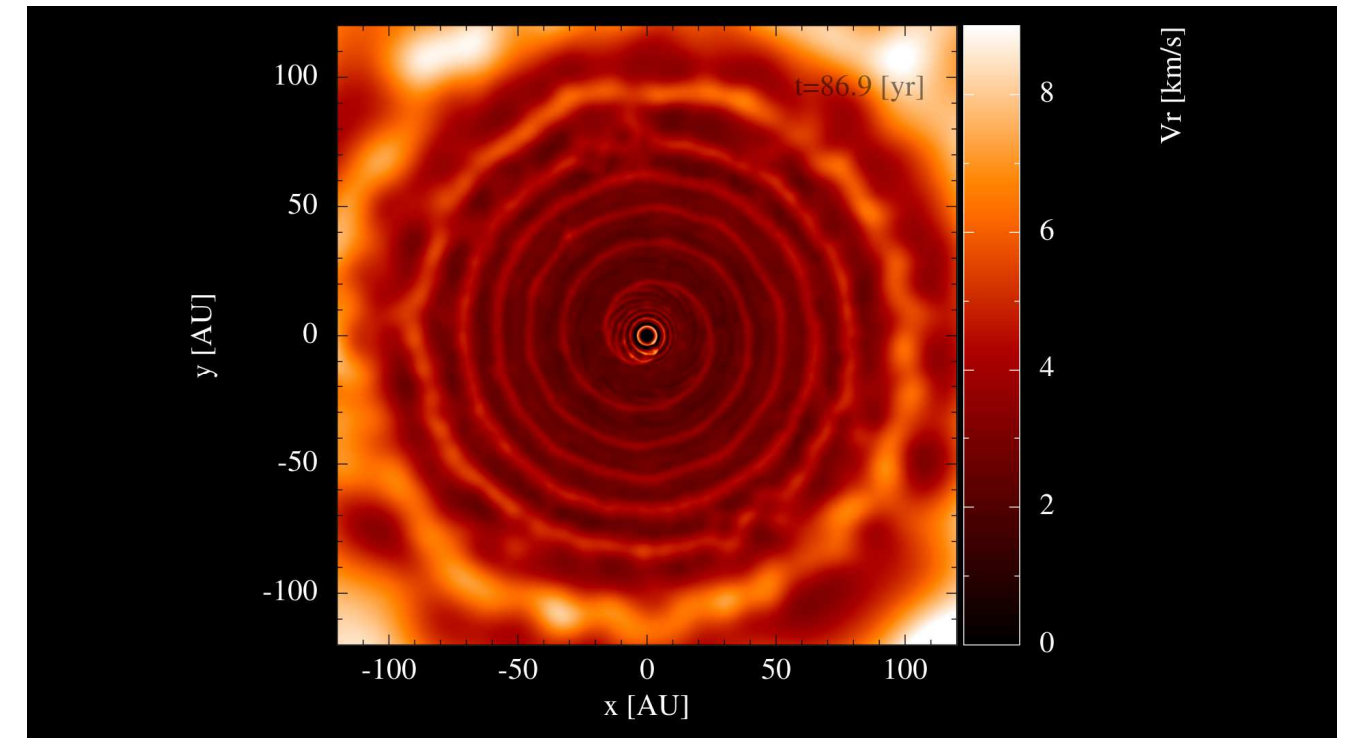
Venue: UWC Zoom

Time: 11h30

Abstract: Understanding the selection biases introduced by AI models in scientific analysis and extracting well-calibrated uncertainties on machine learning outputs are two key challenges facing the systematic use of such algorithms in radio astronomy. In this talk I will discuss our recent work on uncertainty calibration for radio galaxy classification and how these uncertainties can reveal the effects of bias in model outputs, as well as how data curation in astronomy catalogues can cause likelihood

The results of the simulations also show that if the companion travels around the star at a more extended orbit, it forms a single spiral structure created by its wake, but punctuated by undulations due to the pulsations.

Fig. 2 If the companion ends up far enough from the star, a spiral with a single arm would be seen. Credit: Elias Aydi/MSU



The team used the smoothed particles hydrodynamic method, a computational method used to simulate the mechanics of fluid flows, to produce the simulations and simulate the interaction between the stellar pulsations with the nearby companion. This is the first time such simulations are done in 3D and it took weeks, up to months of computational time to run each one of these simulations on a super-computer. A super-computer or a computer cluster is the equivalent of \sim hundreds of computers working together, performing calculations to solve the fluid equations. If we ran these simulations on a normal, commercial laptop or desktop instead, we would have to wait thousands of years for an answer.

When our Sun runs out of fuel in its core and turns into a giant, pulsating star, the stellar pulsation might interact with the giant, gaseous planets in our solar system, such as Jupiter. The team suggests that if Jupiter ends up in a nearby orbit around the future giant Sun and if there is a resonance between Jupiter's orbital period and the solar pulsations, multiple spiral structures might form around the Sun. If Jupiter ends up in an extended orbit around the Sun, a single spiral arm might form.

While such multiple spiral structures have not yet been observed, single spiral structures have been observed frequently around red giant stars, but these are due to the interaction of the star with a more massive, binary **star** companion in a very wide orbit dozens of times the distance Sun-Earth. However, the team hopes that with current and future high-resolution and high-sensitivity facilities such as the Atacama Large Millimeter/submillimeter Array (ALMA) in Chile or the recently launched NASA's James Webb Space Telescope (JWST), we might start observing such multiple spiral structures around giant, evolved stars.

Megamaser “Nkalakatha” discovered by astronomers using MeerKAT

Using the MeerKAT radio telescope, a team of researchers from the University of the Western Cape, the University of Cape Town, Rhodes University, the South African Radio Astronomy Observatory and the South African Astronomical Observatory together with colleagues from 12 other countries have discovered a powerful megamaser - a radio-wavelength laser indicative of colliding galaxies. This is the most distant such megamaser found so far.

Galaxies are vast islands of matter in the universe. They are made of hundreds of billions of stars, gas and dark matter. When galaxies merge in collisions of cosmic proportions, the gas they contain becomes extremely dense. In particular, this can stimulate hydroxyl molecules, made of one atom of oxygen and one atom of hydrogen, to emit a specific radio signal called a maser (a maser is like a laser but emits radio waves instead of visible light). When that signal is exceedingly bright, it is called a megamaser. When two galaxies like the Milky Way and the Andromeda Galaxy collide, beams of light shoot out from the collision and can be seen at cosmological distances. The OH megamasers act like bright lights that say: here is a collision of galaxies that is making new stars and feeding massive black holes, explained Prof. Jeremy Darling from the University of Colorado in the United States, a megamaser expert and co-author of the study.

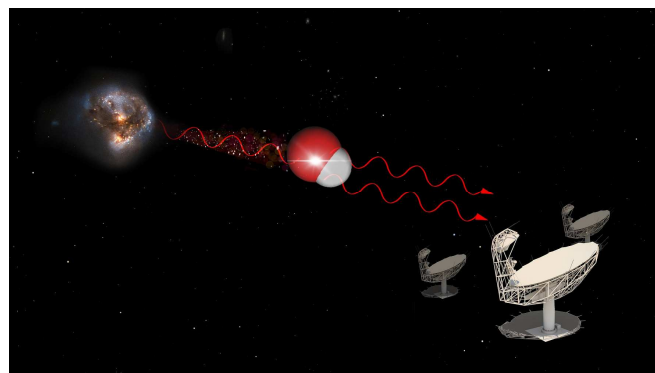


Fig. 1 *Artist's impression of a hydroxyl maser. Inside a galaxy merger are hydroxyl molecules, composed of one atom of hydrogen and one atom of oxygen. When one molecule absorbs a photon at 18cm wavelength, it emits two photons of the same wavelength. When molecular gas is very dense, typically when two galaxies merge, this*

Webinars

Colloquia and Seminars use form an important part of a research facility, often as a sort of pre-publication discussion or a discussion of an individual's current research, and as such it is virtually impossible to “publish” this material. However by recording the topics discussed in the form below does indicate to those, who are unable to attend, what current trends are and who has visited to do research: it keeps everyone ‘in the loop’ so to speak

These form an important part of a research facility, often as a sort of pre-publication discussion or a discussion of an individual's current research, and as such it is virtually impossible to “publish” this material. However, by recording the topics discussed in the form below does indicate to those, who are unable to attend, what current trends are and who has visited to do research: it keeps everyone ‘in the loop’ so to speak

With the advent of CV19, these Colloquia and Seminars are being presented to wider audiences via Zoom and other virtual platforms. The editor has started by identifying what would originally been “local” Colloquia and Seminars; not easy as there are now Webinars on interesting topics from around the globe! In time we will either return to the traditional Colloquia and Seminars or many will become Hybrid session.

Title: Recent advances in Fast Radio Burst studies from the CHIME/FRB telescope

Speaker: Dr. Shriharsh Tendulkar Dept of Astronomy and Astrophysics Tata Institute of Fundamental Research, Mumbai and National Centre for Radio Astrophysics, Pune

Date: 3 March

Venue: SAAO - Zoom

Time: 11h00

Abstract: Fast Radio Bursts (FRBs) are millisecond-timescale radio transients originating from cosmological distances (~Gpc) that have been discovered a little more than a decade ago. At these distances, they have to be a trillion times more luminous than the brightest radio pulses observed from Galactic pulsars. The engine and emission mechanism that can produce such luminosities is still unknown despite ~80 different theories. Over the past few years, the Canadian Hydrogen Intensity Mapping Experiment (CHIME) FRB backend has detected hundreds of FRBs including a dozen repeating FRBs and a few of the nearest FRB sources. The repeating nature of these FRBs, allows for precise localization with radio interferometers and a detailed study of their environment and nature with multi-wavelength observations. I will introduce the broad questions about the nature of FRBs and their promise as tools for cosmology. I will discuss recent results from the CHIME/FRB backend and the inferences that we can draw about the origins of FRBs. Apart from radio observations, I will discuss X-ray and optical studies of FRB locations and the search for prompt counterparts of FRBs. I will finish by discussing the ongoing efforts of the CHIME/FRB collaboration to build outrigger telescopes for FRB localization and our plans at

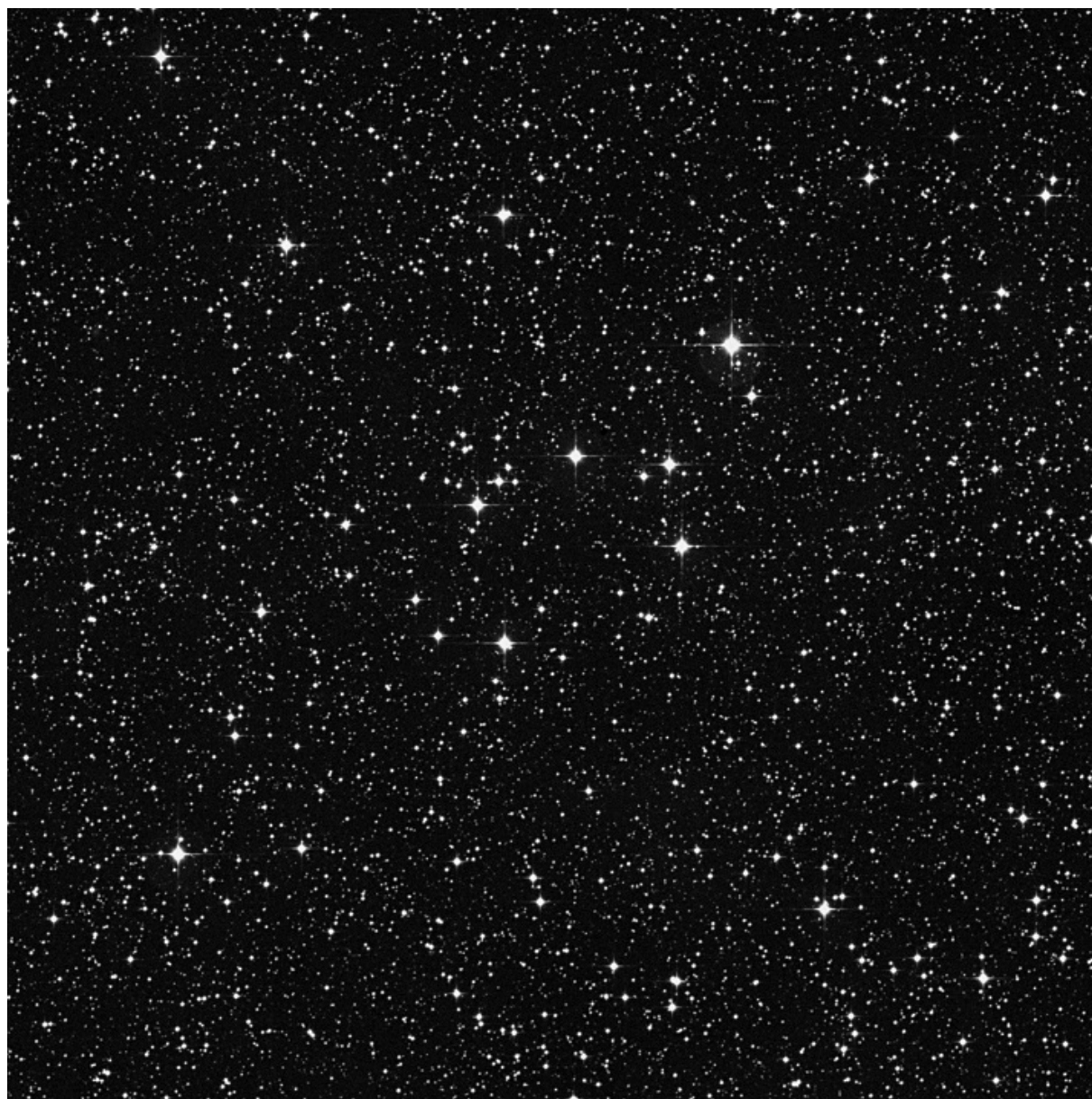
Picture Credit: <http://archive.stsci.edu/cgi-bin/dss>

STREICHER 80 – J0723.3-1237

Canis Major

A dozen stars somewhat brighter than the background star field, situated between the large open cluster NGC 2374 and small compact grouping Haffner 8. It has become a habit of mine to name an object according to the very first thought that strikes me. Although perhaps part of a busy star field the grouping reminds me of a teardrop shape in a way.

OBJECT	TYPE	RA	DEC	MAG	SIZE
STREICHER 80 DSH J0723.3-1237	Asterism	07h23m.20	-12°37'.36	9.5	8.5'



Picture Credit: <http://archive.stsci.edu/cgi-bin/dss>

emission gets very bright and can be detected by radio telescopes such as the MeerKAT. © IDIA/LADUMA using data from NASA/StSci/SKAO/MoIView.

Hydroxyl megamasers emit light at a wavelength of 18cm. This light belongs to the radio part of the electromagnetic spectrum, and it is the type of light that the MeerKAT radio telescope in the Karoo is designed to capture exceptionally well.

The **Looking at the Distant Universe with the Meerkat Array (LADUMA)** team leads one of the big MeerKAT science experiments, which is looking for neutral hydrogen gas in galaxies in one area of the sky, and looking for it very deeply - meaning very far from us, both in space and in time. By measuring the neutral hydrogen gas in galaxies from the distant past to now, LADUMA will contribute to our understanding of the evolution of the universe. This is no minor exercise, and so the research team comprises scientists from South Africa, Australia, Chile, France, Germany, India, Italy, Japan, the Netherlands, South Korea, Spain, the UK, and the US. Associate Professor Sarah Blyth from the University of Cape Town said that LADUMA is probing hydrogen within a single ‘cosmic vuvuzela’ that extends to when the universe was only a third of its present age.

To look for hydrogen, the team looks for light with a wavelength of 21cm that has been stretched to longer wavelengths by the expansion of the universe. However, light from other atoms and molecules is also present, and in their very first observation with MeerKAT, the team detected bright emission from hydroxyl molecules that had been even more stretched from its original wavelength of 18cm. Dr. Marcin Glowacki, previously a researcher at the Inter-University Institute for Data-Intensive Astronomy (IDIA) and University of the Western Cape, and now based at the Curtin University node of the International Centre for Radio Astronomy Research (ICRAR), led the investigation.

He explained that it’s impressive that in a single night of observations with MeerKAT, already found a redshift record-breaking megamaser. The full 3000+ hour LADUMA survey will be the most sensitive of its kind. When they saw this signal in the data coming from the telescope, and confirmed that it was coming from hydroxyl, the team realised that they had a megamaser on their hands.

To make this discovery, the team had to run complex scientific algorithms on large amounts of data. This was made possible by the Inter-University Institute for Data Intensive Astronomy (IDIA) research cloud computing facility. This facility exists to help the South African research community do as much science as possible with the MeerKAT, and with the upcoming Square Kilometre Array in the future. Indeed, it is one thing to collect a lot of data, and another to work with it.

Facilities like IDIA’s are imperative if astronomers are to do as much science as possible with the MeerKAT, and with the Square Kilometre Array in the future.

Once the team knew it was a megamaser, they went on to look for its host galaxy. Where was the megamaser coming from? The patch of sky explored by the LADUMA team has been observed in X-rays, optical light and infra-red, so the team was able to easily identify the host galaxy. The team also knew that such a powerful, distant megamaser needed a good nickname, and invited members of the public to offer suggestions. The winning suggestion was “Nkalakatha,” an isiZulu word that means “big boss,” which was suggested by Zolile Tibane, a student from Johannesburg who is studying computer science at the University of the Western Cape.

The host galaxy of “Nkalakatha” is known to have a long tail on one side, visible in radio waves. It is about 58×10^{21} kms away, and the megamaser light was emitted about 5 billion years ago when the universe was only about two thirds of its current age. Follow-up observations of the megamaser have already been planned, and as LADUMA progresses many more discoveries will be made, noted Dr. Glowacki.

This is the first time a megamaser has been detected at that distance from its emission at 18cm wavelength. The authors of the study point out that it is not surprising that they found such a bright megamaser, given how powerful the MeerKAT is, but the telescope is very new, so this find hopefully is one of many more to come. MeerKAT will probably double the known number of these rare phenomena. Galaxies were thought to merge more often in the past, and the newly discovered OH megamasers will allow us to test this hypothesis, said Prof. Darling.

Radio astronomy is entering a truly exciting time with the upcoming Square Kilometre Array and its pathfinder telescopes, including MeerKAT. Unplanned discoveries are starting to emerge from the unprecedented amounts of data these instruments collect. And with MeerKAT and IDIA, South Africa is right at the cutting-edge of astronomy.

Picture Credit: <http://archive.stsci.edu/cgi-bin/dss>

STREICHER 79 – J0454.7-2854

Caelum

An example of a typical string of relatively bright stars, threading along from north to south. The stars are mainly yellow-coloured, with a faint double star to end off the string towards the north. The open spiral galaxy PGC 16305 is situated only 8’ further north and can barely be seen towards the top left corner in the Deep Sky Survey photograph. Half a degree further north-east, however, the slightly brighter galaxy IC 2106 takes its home.

OBJECT	TYPE	RA	DEC	MAG	SIZE
STREICHER 79 DSH J0454.7-2854	Asterism	04h54m.42	-28°54’.54	10	15.5’



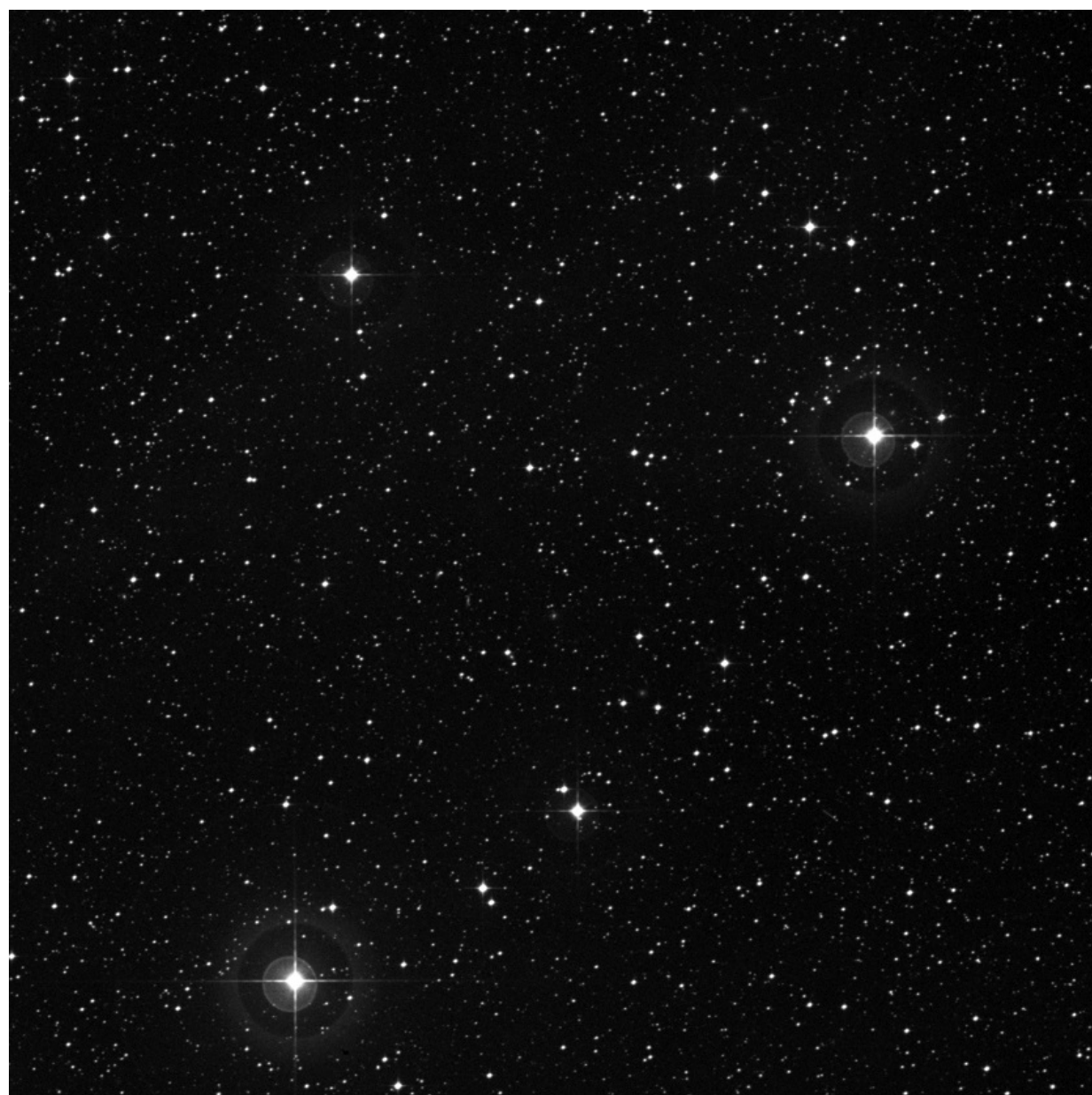
Picture Credit: <http://archive.stsci.edu/cgi-bin/dss>

STREICHER 78 – DSH J1949.5+2833

Vulpecula

The focus is the bunch of faint stars towards the north and east of the star on the right-hand edge (north-west) as seen in the Deep Sky Survey photograph, with fainter stars faltering towards the brighter HD 187640 star on the southern tip. Further in the north-eastern field the beautiful open cluster NGC 6834 and much fainter planetary nebula NGC 6842 can be spotted with a keen eye.

OBJECT	TYPE	RA	DEC	MAG	SIZE
STREICHER 78 DSH J1949.5+2833	Asterism	19h49m.34	+28°33'.30	10.5	23.6'



Observations and images of Comet C/2021 A1 (Leonard)

Tim Cooper¹ and Kos Coronaios²

¹ Director, Comet, Asteroid and Meteor Section, ASSA,

² Public Outreach and Media Liaison, ASSA.

Introduction

For centuries comets have been held in awe, and despite the fact that their appearances are in no way related to events taking place on our planet, the appearance of a bright comet still creates much excitement. It has been some time since a bright comet was observed from southern Africa, the most recent being comet C/2006 P1 (McNaught) which peaked at magnitude -7 , and was easily visible to the naked eye in early 2007, and comet C/2020 F3 (NEOWISE), which reached magnitude 0 in July 2020 but was poorly placed for us at the time it was at its brightest. Following the discovery of comet C/2021 A1 (Leonard) a full twelve months before perihelion, initial indications were that the comet might reach magnitude 4 at the time of a close approach to Earth on December 12, 2021, and possibly a little brighter around the time of nodal crossing due to forward scattering of sunlight by dust particles. In the event the comet became briefly visible to the naked eye, and as a result of several outbursts exceeded expectations for observers in southern Africa. This article provides a concise record and discussion of observations and images of comet C/2021 A1 (Leonard) received from South African observers.

Discovery and orbit

Comet C/2021 A1 (Leonard) was discovered by Gregory Leonard at Mount Lemmon Observatory on January 3.54 UT (Green 2021). At the time it was a magnitude 19 object located in northern Boötes, at distance 5.077 astronomical units (au) from the sun. Preliminary orbital elements showed the comet travelling in a near-parabolic, retrograde orbit (inclination, $i = 132.686$) with perihelion on 2022 January 3.29 at perihelion distance, $q = 0.615$ au. After perihelion the orbit would become hyperbolic (eccentricity, $e = 1.0001$) and the comet will eventually leave the solar system. On its inward journey the comet would make a close approach to Earth on 2021 December 12, 13:54 UT at distance $\Delta = 0.23$ au, followed by a very close approach to Venus of 0.0285 au on 2021 December 18, 02:09 UT. Moreover, Zhang et al (2021) pointed to the fact that Venus would pass within the minimum orbit intersection distance (MOID) of around 50,000 km from the comet's orbit on December 19, leading to the possibility of visible meteors in Venus' atmosphere. From Earth at this time, the comet would be located close to Venus in the evening sky.

Predictions for observability

Following discovery, and during most of 2021, the comet remained faint and too far north for observation from southern Africa. First opportunity to see the comet would

be when it emerged from the solar glare low in the early evening sky around mid-December, by which time it would possibly be a magnitude 5 object in Sagittarius. The actual date the comet would be first sighted was however uncertain, with the light of full moon on December 18/19 expected to interfere. As part of preparations to observe the comet Tim Cooper made a presentation to the Johannesburg Centre of ASSA on December 8, 2021 and outlined what could be expected. Included in that presentation were the predicted observing conditions for Johannesburg as shown in Table 1. Subsequently this Table and a star map showing the position of the comet at various dates were posted on several social media sites.

Date	Comet Altitude °	Comet Azimuth °	Elongation °	Magnitude
December 18	17	248	29	4.7
December 19	20	247	32	4.8
December 20	23	246	34	4.9
December 21	25	246	36	5.0
December 22	26	245	37	5.1
December 23	27	245	38	5.3
December 24	28	245	39	5.4
December 25	29	244	39	5.5
December 26	29	244	39	5.5
December 27	30	244	40	5.6
December 28	30	243	40	5.7
December 29	30	243	39	5.8
December 30	30	243	39	5.9
December 31	29	242	39	6.0
January 1	29	242	38	6.1
January 2	29	242	38	6.2
January 3	28	242	37	6.2
January 4	28	241	37	6.3
January 5	27	241	36	6.4

Table 1 Predicted observing conditions for Johannesburg, all dates for 17h45 UT. Elongation is that of the comet from the sun in degrees. Magnitude is that predicted from equation (2).

The standard brightness equation for comets is:

$$m_1 = H_0 + 5 \log[\Delta] + 2.5n \log[r] + \phi \quad (1)$$

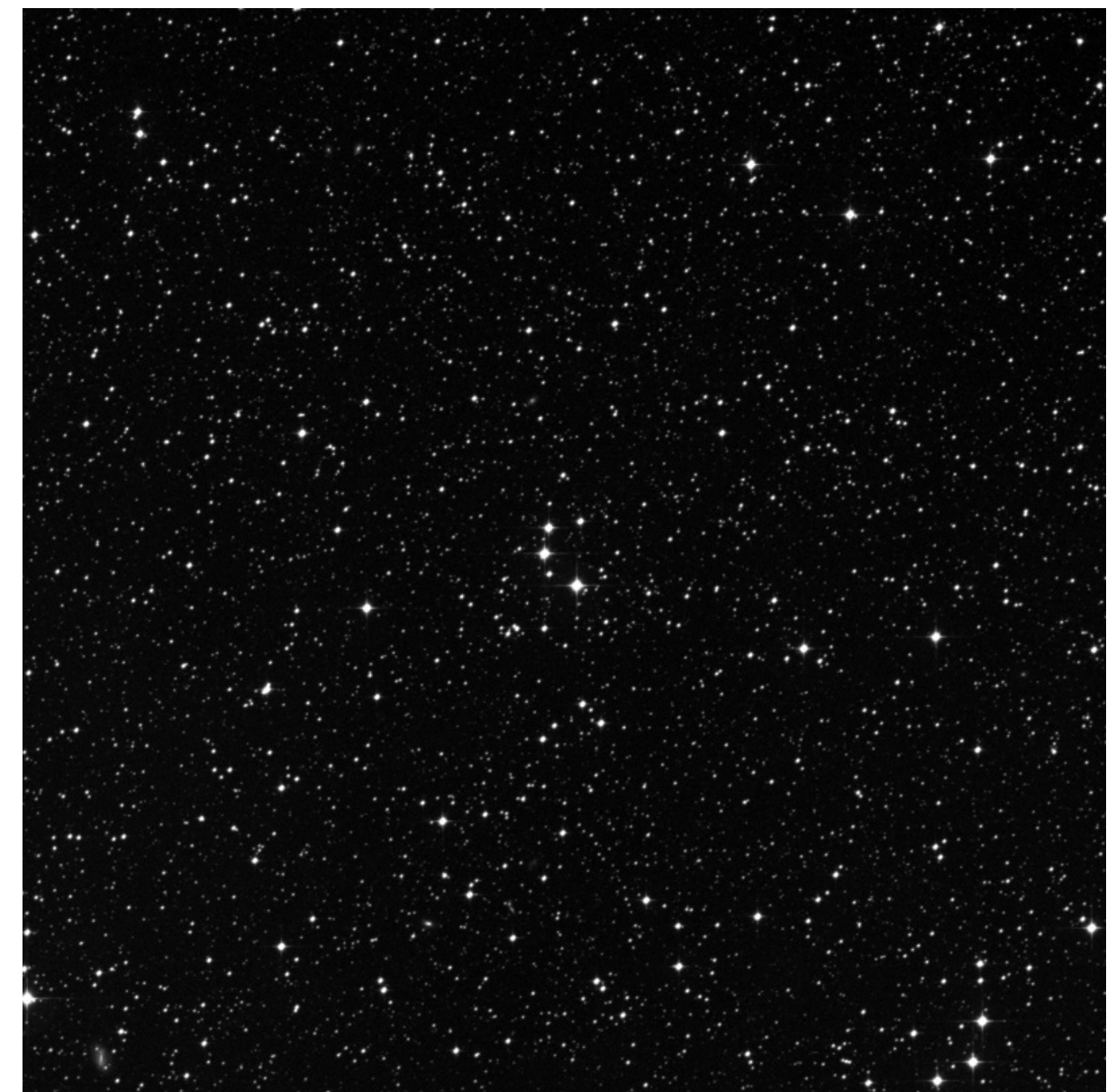
Picture Credit: <http://archive.stsci.edu/cgi-bin/dss>

STREICHER 77 – J1811.4-6247

Pavo

While galaxy hunting in the area around Iota Pavonis I came across this nice tight grouping, consisting of only 5 outstanding stars but strikingly outstanding against the star field. A mist of fainter stars intermingles with well with the brighter stars. The open end of this halfmoon is towards the west with the brightest southern star catalogued as HD 165681.

OBJECT	TYPE	RA	DEC	MAG	SIZE
STREICHER 77 DSH J1811.4-6247	Asterism	18h11m.26	-62°47'.06	9.5	2'



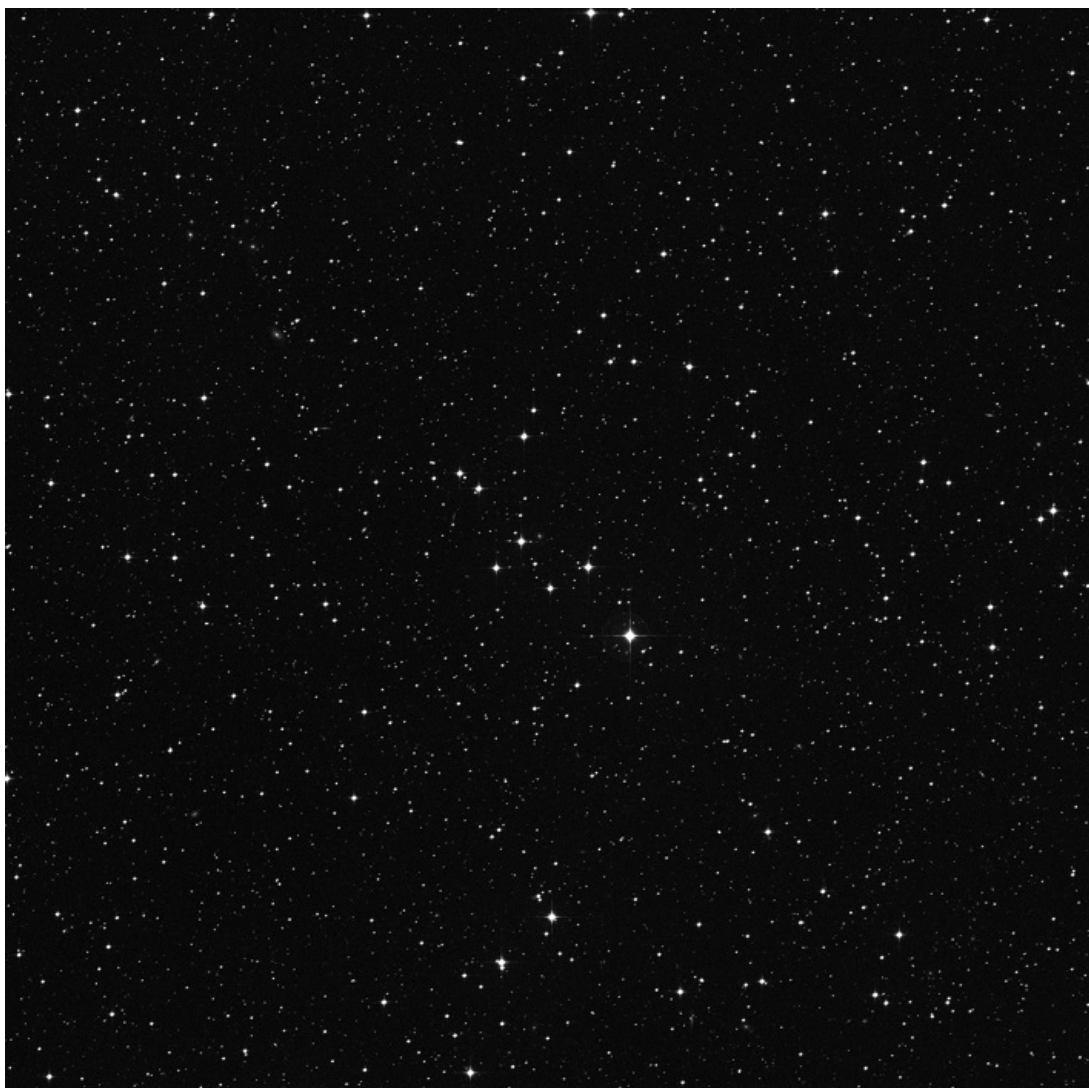
Streicher Asterisms

Magda Streicher

STREICHER 76 – J1329.5-3448 Centaurus

The southern bright magnitude 9 star shows the way to the rest of the grouping towards the north, which is similar in brightness and colour. Seen as a whole the grouping in a north-east to south-west direction is quite outstanding against the fainter background star field. The spiral galaxy NGC 5188 is situated only 20' towards the east.

OBJECT	TYPE	RA	DEC	MAG	SIZE
STREICHER 76 DSH J1329.5-3448	Asterism	13h29m.36	-34°48'.12	10.2	9'



where m_1 is the total cometary magnitude, H_0 is the absolute magnitude of the comet at $\Delta = r = 1$ au, Δ is the geocentric distance of the comet in au, n is the magnitude slope factor, r is the heliocentric distance of the comet in au, and ϕ is a correction for forward scattering of sunlight due to phase angle. Taking the absolute magnitude from the Comet Observation Database (COBS) data as 8.60, slope factor as 4.16, and neglecting forward scatter gave the predicted magnitude according to (2):

$$m_1 = 8.60 + 5 \log[\Delta] + 10.40 \log[r] \quad (2)$$

Magnitudes predicted from this equation were used in Table 1. It can be seen the comet was expected to emerge from the solar glare perhaps as early as December 16, as a magnitude 4-5 object low in the south west in evening twilight. Maximum elongation of 40° would occur around December 27/28, after which the comet would slowly descend towards the horizon again, setting earlier each evening, and becoming unobservable by end of January 2022. Following these predictions, we present actual observations received in this article.

Explanatory notes to features observed in comets

While far from the sun the comet is a frozen nucleus, devoid of any surrounding nebulosity and appears asteroidal, or star-like. As it approaches the sun the nucleus comes under the effects of solar radiation, its volatiles begin to sublimate, releasing gases and dust particles into its environment, and forming a coma around the nucleus. These gases and dust particles are driven away from the coma under the effects of the solar wind and radiation pressure to form the different tails. In this article the various cometary features have the following meanings.

The degree of condensation of the coma (DC) is the existence of a sharp central disk, or sharp brightness intensity gradient within the coma, and is assessed by comparing the visual appearance in the eyepiece with a pre-drawn scale (see Edberg 1983). The scale runs from 0 to 9, with DC = 0 representing a totally diffuse coma without any central brightening; DC = 1, very slight brightening; DC = 3, obvious brightening, but still very diffuse; DC = 5, distinct brightening, described as moderately condensed; DC = 7, sharp brightening, some diffuseness, described as strongly condensed and DC = 9, star or disk-like, with no diffuse coma visible. Coma diameter is measured in arc minutes. In some cases the coma may appear elliptical or irregular. In such cases the dimensions may be recorded individually, or simply state that the coma is elongated in a specific position angle.

Since the coma is a very dynamic environment surrounding the active, rotating nucleus, particularly in the vicinity of perihelion, many features may be observed which change appearance over short time scales. Fountains (Class F features) may be visible emanating from the false (or pseudo) nucleus and may change in intensity as

active sites on the nucleus rotate in and out of sunlight. Various envelopes or hoods (Class H features) may be discerned as bright arcs within the coma. Streamers or jets (Class J features) of gas and dust may appear in the sunward direction which then curve backwards and merge into the tail. In the anti-solar direction, bright spikes or rays (Class R features) may appear, which are formed by ionized gases and are the initial stages of formation of the Type I tail before this is carried away from the coma (Green 1997).

Cometary tails are divided into two types depending on the nature of species that form them. Type I tails are due to ionised gas molecules, mainly ionised carbon monoxide CO^+ , but also N_2^+ , CO_2^+ , CH^+ and OH^+ (Brandt 1968), which are excited by energetic solar radiation and carried away from the coma and align with the magnetic field lines of the charged solar wind. The characteristic blue colour of the tail seen in some images is due to fluorescence of CO^+ at 427.3nm, the so-called Comet Tail Bands. Several distinct features may be discerned within Type I tails; firstly a number of bright rays or filaments, which arrange symmetrically around the tail axis. Individual filaments may show kinks or knots. Of particular interest is the presence of disconnection events, when whole sections of the ion tail appear to detach from the comet, caused by anisotropies in the interplanetary magnetic field (Ip 2004). All of these features are affected by variations in the solar wind and coronal mass ejection events on the sun (Wegmann 2002).

Type II tails are due to solid dust particles, which are released from the nucleus as volatile gases sublimate. Once liberated these dust particles are free to follow their own paths and gradually diffuse away from the coma to form the dust tail. The dust distribution, and ultimately the appearance of the tail depends on a number of factors, including ejection time, particle size, ejection velocity and influence of the solar wind and radiation pressure on the ejected particles. Consequently dust tails may show striations or bands due to particles ejected from the nucleus at the same time (synchronic bands, or synchrones), appearing as radial bands and radiating away from the nucleus. These synchrones were well demonstrated by comet C/2006 P1 (McNaught). Fine structures may also be seen from particles of similar size (syndynes) as spirals tangent to the sun-comet radius vector (Fulle 2004).

The position angle (p.a.) of the tail is the orientation relative to the position on the coma or head of the comet from which the tail emanates. It is measured from an image or plot with celestial north being p.a. = 0° and east being p.a. = 90° , etc. The position angles of all tails, and other features, can be recorded. If the dust tail is curved, then the length can be measured at various position angles.

Ip, H-W., (2004), Global solar wind interaction and Ionospheric dynamics, in *Comets II*, pp609-610, *ibid*.

Larson, S. M. and Sekanina, Z., (1984), Coma morphology and dust-emission pattern of periodic Comet Halley. I - High-resolution images taken at Mount Wilson in 1910, *Astronomical Journal*, **89**, pp 571-578.

Wegmann, R., Large-scale disturbance of the solar wind by a comet, *Astron. Astrophys.*, **389**, 1039-1046.

Zhang Q., Ye Q., Vissapragada S., Knight M. M. and Farnham T. L., (2021), Preview of Comet C/2021 A1 (Leonard) and Its Encounter with Venus, *Astronomical Journal*, **162**, 194.

Figure 28; January 19, 2022, Kos Coronaios, first image taken at 19h17, Canon 60D, 200mm Canon EF lens, f2.8, ISO 1600, 12 x 30 second exposure, cropped.

Figure 32; Gary Deacon, all images with Nikon D5600, December 21, 2021 at 19h12, f/l 300mm, 2 seconds, f/6.3 ISO 6400. December 22 at 19h24, 300 mm, 1.6 seconds, f/6.3 ISO 6400. December 23 at 19h37, 200 mm, 5 seconds, f/5.6 ISO 3200. December 25 at 19h30, 160 mm, 5 seconds, f/6.3 ISO 6400. January 8, 2022 at 19h30, 300 mm, 2 seconds, ISO 5000, stack of 20 images. January 13 at 19h30, 300 mm, stack of 50 images, various shutter speeds from 1.3-2 seconds, ISO 6400, Sequator used for stacking.

Acknowledgements

Orbital elements and close approach data are from Jet Propulsion Laboratory, Small-Body Database Lookup, <https://ssd.jpl.nasa.gov/tools/>, accessed on January 22, 2022. Light curves were generated using data from COBS, credit to COBS Comet Observation Database – CC BY-NA-SA 4.0. Thanks to Dr Nic Erasmus, South African Astronomical Observatory, for facilitating discussion on the colour of the coma, and to Dr Alan Fitzsimmons, Queen's University Belfast, for comments made in that regard.

References

- Behar, E., Nilsson, H., Henri, P., Bercic, L., Nicolaou, G., Stenberg Wieser, G., Wieser, M., Tabone, B., Saillenfest, M. and Goetz, C., (2018), The root of a comet tail: Rosetta ion observations at comet 67P/Churyumov-Gerasimenko, *Astron. Astrophys.*, **616**, doi.org/10.1051/0004-6361/201832842.
- Borsovsky, J., Nauta, K., Jiang, J., Hansen, C. S., McKemmish, L. K., Field, R. W., Stanton, J. F., Kable, S. H., and Schmidt, T. W., (2021), Photodissociation of dicarbon: How nature breaks an unusual multiple bond, *Proceedings of the National Academy of Sciences* **118(52)**, doi.org/10.1073/pnas.2113315118
- Brandt, J. C., (1968) The Physics of Comet Tails, *Annual Review of Astronomy and Astrophysics*, **6**, pp267-286, doi.org/10.1146/annurev.aa.06.090168.001411.
- Edberg, S. J., (1983) in *International Halley Watch Amateur Observers' Manual for Scientific Comet Studies*, Part 1, Methods, pp5-6 and 5-7, Sky Publishing Corporation.
- Feldman, P. D., Cochran, A. L. and Combi, M. R., (2004), Spectroscopic Investigations of Fragment Species in the Coma, in *Comets II*, pp 425-447, edited by Festou, M. C., Keller, H. U. and Weaver, H. A., University of Arizona Press.
- Fitzsimmons, A., (2022), Astrophysics Research Centre, Queen's University Belfast, private communication in email dated January 12, 2022.
- Fulle, M., (2004), Motion of Cometary Dust, in *Comets II*, pp565-566, ibid.
- Green, D. W. A., (1997), in The ICQ Guide to Observing Comets, special issue of the International Comet Quarterly.
- Green, D. W. A., (2021), Comet C/2021 A1 (Leonard), Electronic Telegram No. 4907, Central Bureau for Astronomical Telegrams, issued 2021, January 10.

Chronology and descriptive observations

First observations of the comet were hampered by weather conditions countrywide during December, and the effect of a weak La Niña system coupled with a neutral El Niño-Southern Oscillation (ENSO) ensured long periods of cloud and rain over most areas. The first visual observation of the comet as it emerged from the sun's glare in evening twilight was by Kos Coronaios on December 18, 2021, observing from Pearly Beach, Western Cape. The comet was followed until the last observation on January 19, 2022, also made by Kos. The complete observations received follow according to date. Note abbreviations used are B = binoculars, DC = Degree of Condensation of the coma, a slash following the value indicates a fractional value, so 6/ indicates between 6 and 7, m_1 = total cometary magnitude, p.a. = position angle, RV = radius vector of the tail, T = Schmidt-Cassegrain telescope. Note all times are given in UT.

December 18, 2021 - Easily visible in 10x50B and 12x50B, estimated magnitude around 4.5. Stunning sight in 20cmT. Not visible to naked eye due to light from full moon [KC]. Figure 1 shows a short stubby tail, length 0.4° centred in p.a. 91° , but comet at low altitude [KC].



Fig. 1 December 18, 2021, Kos Coronaios. Star above left is 59 Sgr, and near right edge is ω Sgr.

December 20, 2021 - In 16x50B, detected at 17h43 in bright twilight, then at 17h52, bright, easy, stands out despite thin cloud, well condensed, DC = 8, tail visible but not measured due to cloud, $m_1=3.0$ after correcting for atmospheric extinction [TC]. Figure 2, tail is a narrow fan, length $38'$ spanning p.a. 71° to 103° and centred on p.a. 92° . Coma shows distinctive aqua-blue colour [LS].

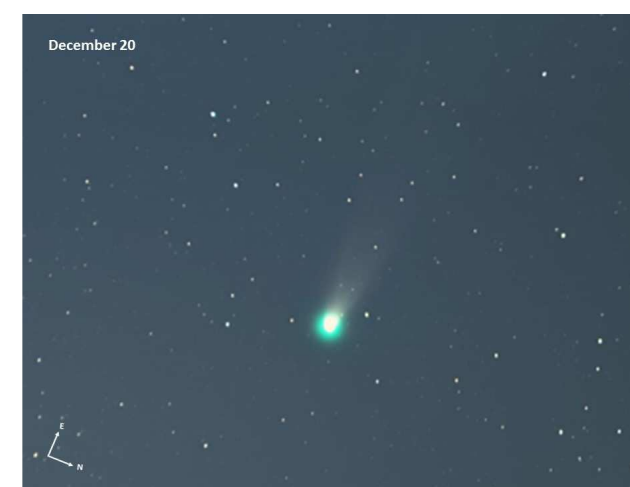


Fig. 2 December 20, 2021, Lafras Smit. Note the colour on the sunward side of the coma. Tail is a narrow fan.

December 21, 2021 - Figure 3, bright condensed round coma, diameter $3'$, surrounded by parabolic hood leading into tail which is a narrow fan, width $8'$, centred on p.a. 93° [GD].

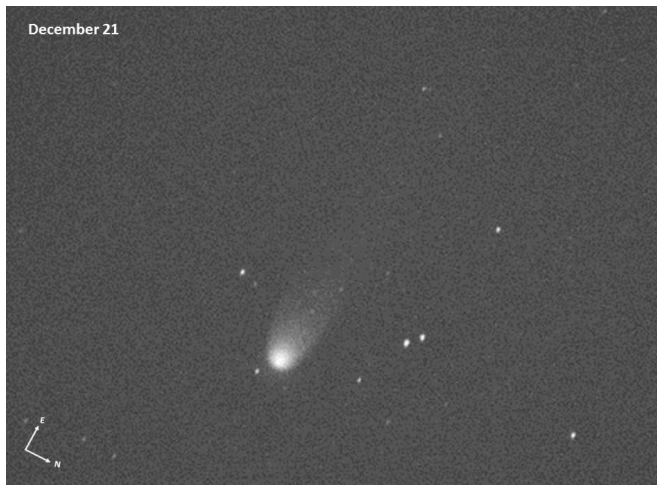


Fig. 3 Image by Gary Deacon, December 21, 2021. The two stars to the right of the comet are SAO 212301 and 212303, and are separated by 2.3'. Short tail is a narrow parabola.

December 22, 2021 – In 16x50B, 18h05, poor sky, hazy after earlier cloud cleared, much fainter than previous, $m_1=4.6$, DC = 6/ [TC]. Figure 4, left panel shows distinct class R spike, length 3' in p.a. =

94°. Tail is a narrow fan, length >0.5° centred on p.a. 94°, and extends beyond the field of view. Note the blue-green colour of the coma on the sunward side, Right panel converted to negative and contrast enhanced to reveal features, condensed central coma surrounded by parabolic envelope [PL].

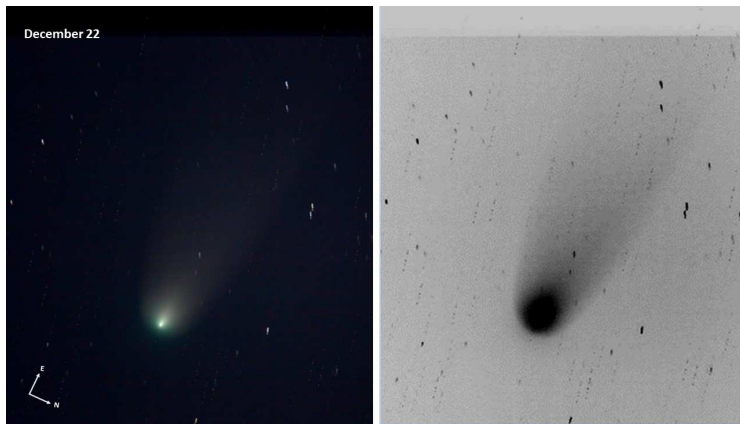


Figure 4 December 22, 2021, Paul Ludick. Evening prior to outburst. Positive image shows evidence of a sharp spike leading into the tail. Contrast enhanced negative image, tail is a narrow parabola.

December 23, 2021 - Comet is in outburst! 16 x 50B, $m_1=3.5$, coma is

smaller than previous but more condensed, DC = 8, and narrow fan-shaped tail. In 30 cmT x 110, remarkable! Considerable bright coma surrounding a sharp bright bar which appears biconvex in shape and oriented perpendicular to the tail direction [TC]. Comet visible to the naked eye at 19h30, estimated magnitude about 3.5, about half a magnitude brighter than yesterday [KC]. Figure 5, contrast enhanced, shows the appearance of the comet during outburst in a dark sky, tail is a narrow fan, length 1.6°, brightest in p.a. 89° and slightly curved at the end towards south. The tail on its northern side is clearly brighter [HM].

Fig. 5 Image by Hannetjie Minnaar, December 23, 2021, gives a good idea of the binocular appearance of the comet just after twilight



20h18 same camera settings, 20 second exposures, 11 images stacked, 7 dark frames subtracted and enhanced in Lightroom.

Figure 15; December 27, 2021, Angus Burns, stack of 40 x 4 seconds exposures at 18h10, Canon 5D mark IV on static tripod, EF 70-300mm f4-5.6 IS II USM, image taken at 151mm f5.6, ISO 6400. No calibration, stacked in DSS and processed in LR/CC2019.

Figure 16; December 27, 2021, Kos Coronaios, first image taken at 19h27, Canon 60D, 200mm Canon EF lens, f2.8, ISO 3200, 14 x 40 seconds exposures.

Figure 17; December 28, 2021, Tiaan Niemand, Celestron RASA 11" Telescope, iOptron CEM60EC Mount, ZWO ASI1600mc-cool Camera. 127 frames of 9 seconds each. 18h25-18h52. -10°C sensor temperature. Data captured using SharpCap, dark and flat calibration and stacking with Pixinsight. Processing done in Pixinsight with final touches in Photoshop.

Figure 18; December 28, 2021, Angus Burns, stack of 38 x 45 second exposures from 18h13, Canon 60Da at ISO 1600 on Redcat51 250mm f4.9 telescope, Baader Neodymium skyglow filter, CGEM mount. No calibration, stacked using APP and finished in LR/CC2019.

Figure 19; December 29, 2021, Angus Burns, stack of 64 x 30 seconds exposures from 18h18, ZWP294mc Pro camera on Redcat51 250mm f4.9 refractor, Baader Neodymium skyglow filter. No calibration, stacked using APP and finished in LR/CC2019.

Figure 20; December 29, 2021, Lafras Smit, Sky-Watcher 10 inch f/4.7 reflector, Sky-Watcher EQ6 mount, Canon 90D, ISO 3200, stack of 10 x 30 seconds exposures, first at 18h05. Stacked with Sequator and processed with Photoscape X.

Figure 21; December 30, 2021, Tim Cooper, sketch of observation with 30cm f/10 Meade LX90 SCT, x120, 18h05-18h24.

Figure 22; December 31, 2021, Kos Coronaios. Left hand panel, 19h18, Canon 60D, 200mm EF lens, f/2.8, stack of 15 x 30 seconds exposures, ISO1600. Right hand panel, January 1, 2022, 19h25, Canon 60D, 200mm EF lens, f/2.8, stack of 31 x 40 seconds exposures, ISO1600.

Figure 23, December 31, 2021, Chantal Fourie, Nikon D5300, 300mm f/5.6, stack of 89 x 2 seconds exposures at ISO 10000, between 19h02-19h09, post-processed in DeepSkyStacker, Photoshop and Lightroom.

Figure 24; January 1, 2022, Magda Streicher, sketch of observation with 40cm f/10 Meade LX200 SCT, x100 and x240, 17h15-18h22.

Figure 25; January 4, 2022, Kos Coronaios, image taken at 20h17, Canon 60D, Canon EFS 18-135mm, set at 53mm, f/5, ISO 6400, single 60 seconds exposure.

Figure 26; January 4, 2022, Kos Coronaios, image taken at 19h45, Canon 60D at prime focus on 20cm f/10 SCT, ISO 6400, 30 seconds exposure.

Figure 27; January 8, 2022 Oleg Toumilovitch at 18h10, Celestron 20cm XLT SCT with x0.63 focal reducer, Canon EOS550D, single 4 second exposure at ISO 3200, unprocessed.

Niemand, Alberton, Gauteng; WF = Wim Filmalter, Riversdale, Western Cape; WK = Willie Koorts, Wellington, Western Cape.

Exposure details of images

Figure 1; December 18, 2021, Kos Coronaios, Canon 60D, 200mm Canon EF lens, f2.8, ISO 800, 10 second exposure at 18h59, levels adjusted.

Figure 2; December 20, 2021, Lafras Smit, Canon 90D, 70-200mm lens set at 200mm, f/2.8 on a normal tripod. ISO 6400, stack of 10 x 3 seconds exposures, first at 18h03. Stacked with Sequator and processed with Photoscape X. Bright moon interfered.

Figure 3; December 21, 2021, Gary Deacon, 19h12, Nikon D5600, 300mm, f/6.3, 2 second exposure at ISO 6400

Figure 4; December 22, 2021, Paul Ludick, Canon EOS5 DMKIII, prime focus on Celestron CPC800, ISO 3200, 9 x 3.9 seconds exposures stacked, contrast and brightness adjusted.

Figure 6; December 23, 2021, Kos Coronaios, first image taken at 19h39, Canon 60D, 200mm Canon EF lens, f2.8, ISO 6400, stacked 65 x 3.2 seconds exposures.

Figure 7; December 23, 2021, Wim Filmalter, Nikon D5100 at ISO 6400 ISO, prime focus on homebuilt Jaegers Optics 110mm f4.5 refractor, single 15 seconds exposure at 18h20, homebuilt tracking platform.

Figure 8; December 23, 2021, Willie Koorts, Canon EOS 100D, 85mm f/1.8 lens. Stack of images, processed in Lightroom.

Figure 9; December 22, 2021, Oleg Toumilovitch, left hand panel at 18h11, Celestron 8" XLT SCT with x0.63 focal reducer, Canon EOS550D, single 6 seconds exposure at ISO 1600, unprocessed. December 23, 2021, right hand panel at 17h39, Celestron Onyx-80 f/6.25 ED refractor, Nikon D7000 DSLR, single 6 second exposure at ISO 2000, unprocessed.

Figure 10; December 24, 2021, Lafras Smit, Canon 90D, 70-200mm lens set at 200mm, f/2.8 on a normal tripod, ISO 8000, stack of 60 x 3 seconds exposures, first at 18h15. Stacked with Sequator and processed with Photoscape X.

Figure 11; December 24, 2021, Tiaan Niemand, Celestron RASA 11" Telescope, iOptron CEM60EC Mount, ZWO ASI1600mc-cool Camera. 124 frames of 2 seconds each. 17h55-18h09. -10°C sensor temperature. Data captured using Sharpcap, dark and flat calibration and stacking with Pixinsight. Processing done in Pixinsight with final touches in Photoshop.

Figure 12; December 24, 2021, Oleg Toumilovitch, Nikon D7000, ISO2500, on 8"XLT SCT, single 6 seconds exposure at 20h16, unprocessed.

Figure 13; December 24, 2021, Tim Cooper, 30cm Meade LX90 SCT. Starlight Xpress SXV-M7 camera, 2x2 binning, single 5 second exposure, uncalibrated, Larson-Sekanina filter applied in Astroart 5.0.

Figure 14; December 26, 2021. Johan le Roux. Left panel at 20h06, Canon EOS 100D, 85mm f/1.8, ISO800, 15 seconds exposures, 36 images stacked using Sequator, 6 dark frames subtracted, image enhanced in Lightroom. Right panel negative image, at

Figures 6-8 show the comet during outburst in more detail. Figure 6, bright condensed coma, aqua blue colour distinctive on sunward side, narrow fan shaped dust tail extending 1.5° in p.a. 94°. Two distinct ion features in p.a. 89° and 95°, the former is more prominent and leads to the tail appearing brighter on its northern side [KC].

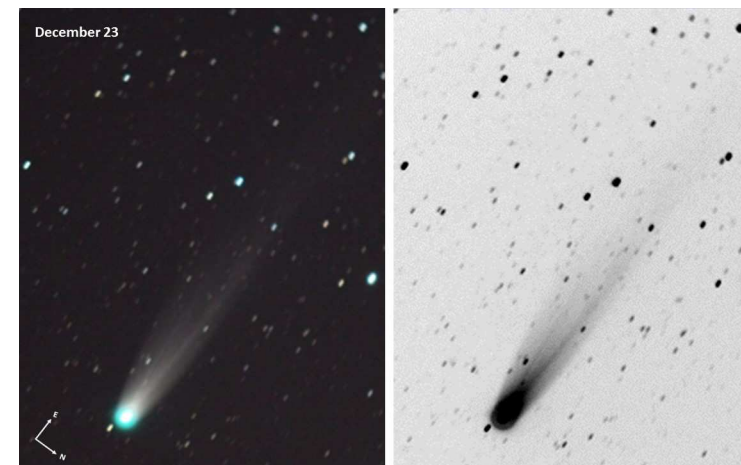


Fig. 6 December 23, 2021, Kos Coronaios. The spike seen in Figure 4 has now developed into a bright ion tail. Bright star at right edge is γ Microscopii, mag. 4.7.

Figure 7 surprise clear sky gave some opportunity to image the comet. Tail is a narrow parabola centred on p.a. 94°. Two or three ion filaments, brightest on the northern side of the tail and visible for 1.0° in p.a. 90°. Could not detect with naked eye [WF]. Two of the ion filaments also show up well in Figure 8 [WK].

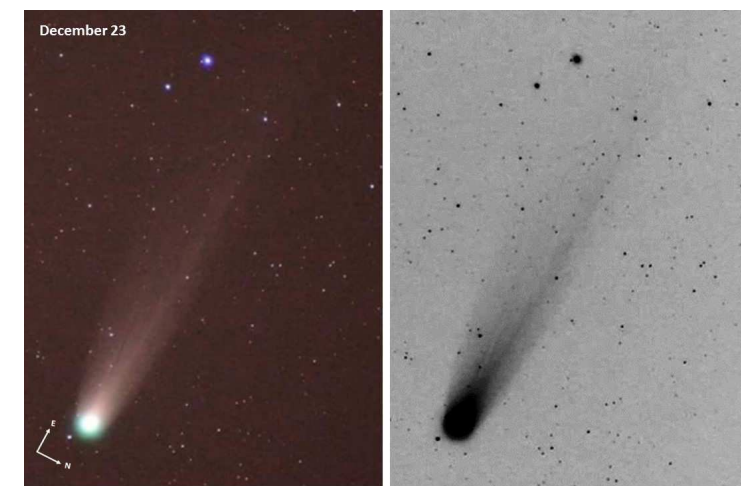


Fig. 7 December 23, 2021, Wim Filmalter, showing three distinct ion filaments

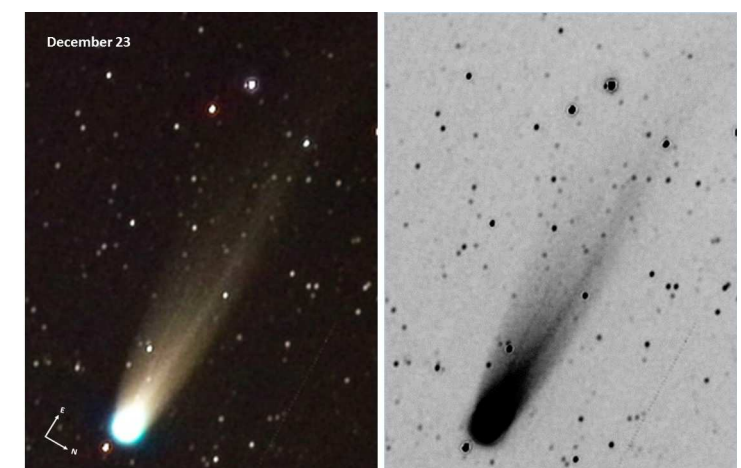


Fig. 8 December 23, 2021, Willie Koorts.



Fig. 9 December 22 and 23, 2021, Oleg Toumilovitch. Note the difference in appearance of the inner coma and false nucleus. The image on the right is after the outburst in activity.

Figure 9, shows the appearance of the inner coma, and the dramatic change that took place in appearance between December 22 and 23. Note the similarity in appearance of the comet on December 21 (Figure 4) and December 22, while the image for December 23 clearly shows the shape of the false nucleus and inner coma after the outburst, with two bright jets curving along the northern and southern sides into the tail. ‘This was a very special evening. I aimed telescope at the comet and noticed that it appears to be much brighter and larger than I was expecting it to be. As soon as the image was taken I realised that the comet was experiencing quite a dramatic outburst’ [OT].

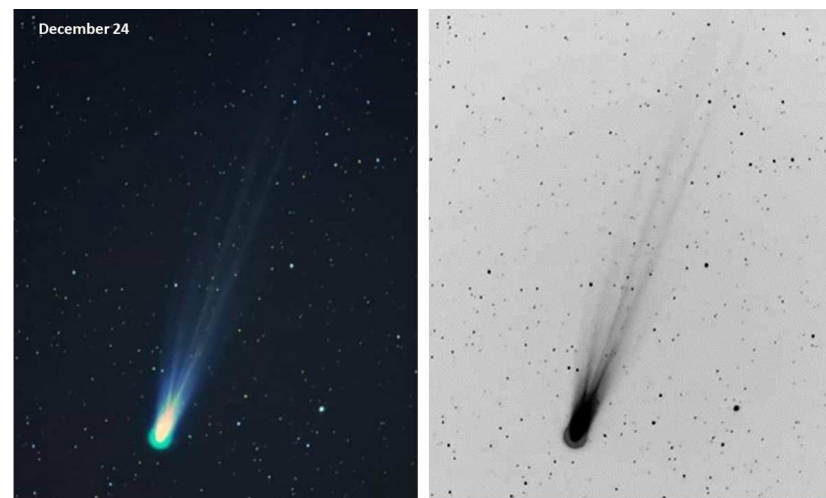


Fig. 10 December 24, 2021, Lafras Smit, showing significant development of ion filaments 24 hours after outburst.

December 24, 2021 - Observed at 18h15, 16x50B, very slightly fainter than last night, $m_1 = 3.7$, DC = 7 [TC]. Figure 10 shows how the three ion features have become more prominent one day after outburst. Brightest is towards the northern side, length 2.9° in p.a. 86° . Coma distinctive aqua-blue colour [LS].

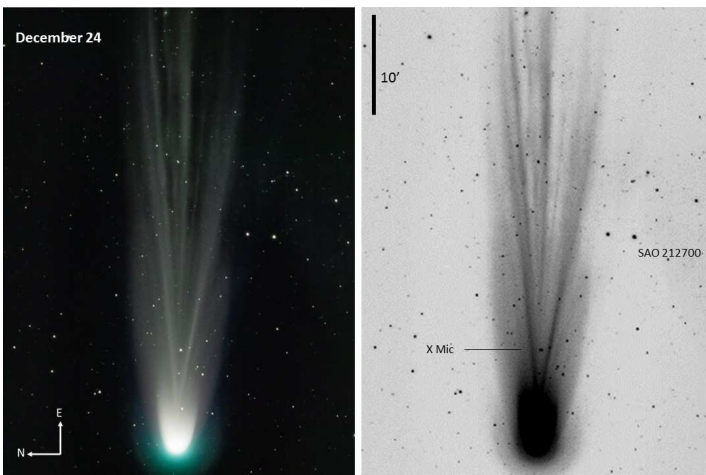


Fig. 11 December 24, 2021, Tiaan Niemand. The star between two filaments is the Mira type variable star X Microscopii.

Figure 11, comet low in the west just after sunset, managed to capture before the comet disappeared behind

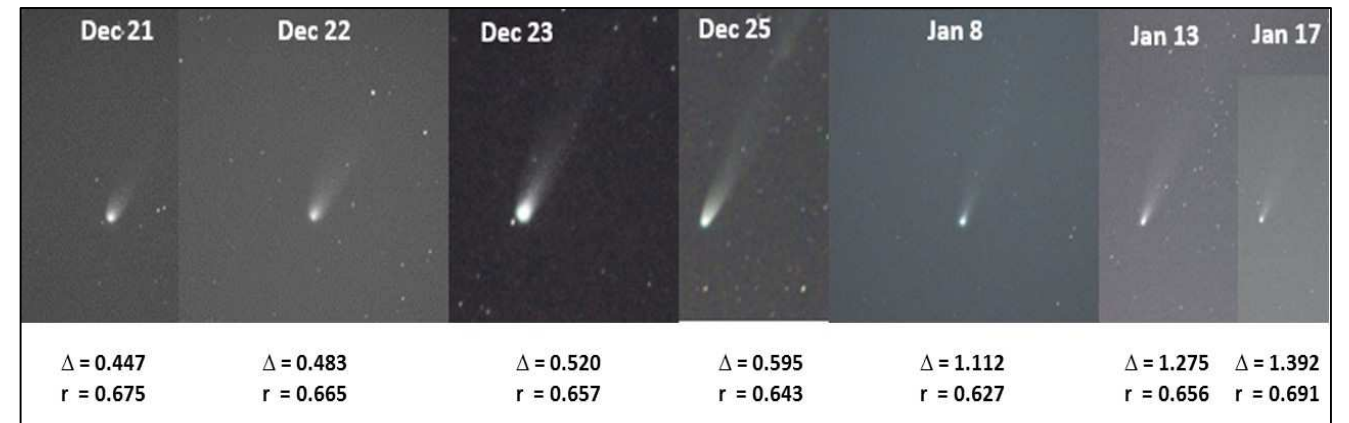


Fig. 32 sequence of images by Gary Deacon between December 21, 2021 and January 17, 2022, showing the changing appearance of the comet. Images have been resized to about approximately the same scale, and intend to show the overall appearance of the comet in the evening sky. Geocentric distance increases from left to right, heliocentric distance is at its smallest in the fifth frame, which is five days after perihelion ($r = 0.615$).

Summary

Comet C/2021 A1 (Leonard) put on a fine performance as seen from South Africa. It was first observed on December 18, 2021, visible low in the west in bright twilight, and was last observed on January 19, 2022, a period of 33 days under observation. Following a number of outbursts the comet peaked at about magnitude 3.0, was easily visible in binoculars and was briefly visible to the naked eye. The coma was strongly condensed, elongated and distinctly coloured in images around the time of perihelion. Colour was detected visually in large telescopes. The tail length exceeded 6° in images, and 3° in binoculars. The ion tail showed complex activity following the outburst on December 23, including a disconnection event on December 26. The comet was seen by many members of the public, was observed visually by several ASSA members, and these together with many excellent images enabled this analysis. This report provides a concise record of observations received, and discussion of the results derived therefrom. Included is some background to the types of features observed, and hopefully gives some pointers on what observations are required for future comets.

Key to observers

AB = Angus Burns, Newcastle, KwaZulu Natal; CF = Chantal Fourie, Danabaai, Western Cape; GD = Gary Deacon, Noordhoek, Western Cape; HM = Hanneljie Minnaar, Gauteng; JIR = Johan le Roux, Western Cape; KC = Kos Coronaios, Pearly Beach, Western Cape; LS = Lafras Smit, Kroonstad, Free State; MS = Magda Streicher, Polokwane, Limpopo; OT = Oleg Toumilovitch, Victory Park, Gauteng; PL = Paul Ludick, Hartbeespoort Dam, Gauteng; TC = Tim Cooper, Bredell, Gauteng; TN = Tiaan

The Type I (ion) and Type II (dust) components were generally coincident, with the ion tail always being within the confines of the dust tail. It might be expected that the Type I tail is aligned with the anti-solar radius vector, but this is not always the case, and generally a small deviation (ϵ) exists (Brandt 1968). We measured the position angles (p.a.) of the tail features and compared these to the radius vector (RV) for the respective date. During December, the p.a. of the tail is fairly close to the RV, with ϵ in the region 1-2°. This increased to $\epsilon \sim 8-9^\circ$ by January 8, and wider thereafter, though there were few measurable images after this date. Also there were too few observations to enable determination of any periodicity in the p.a. of the ion tail.

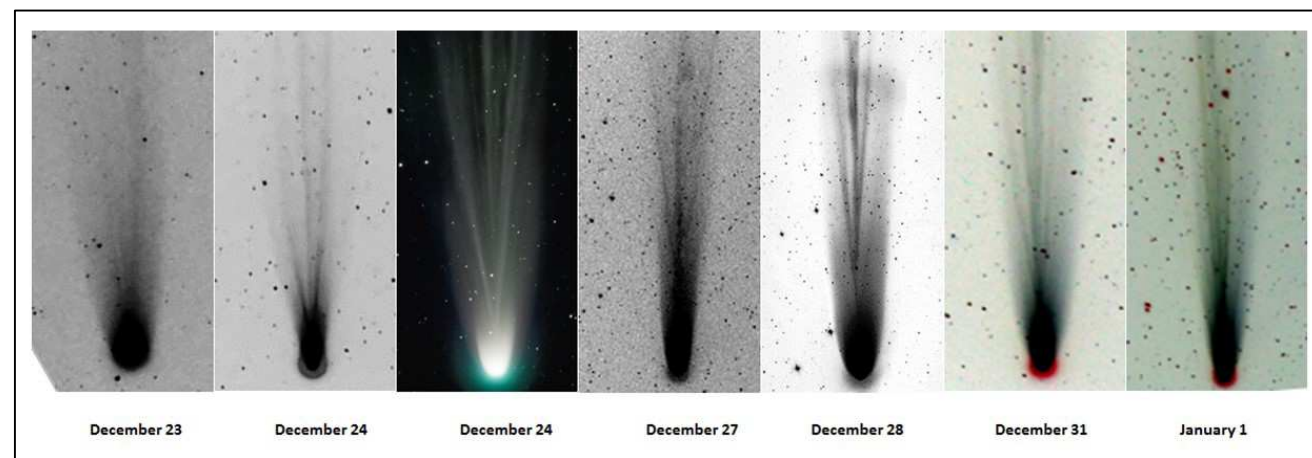


Fig. 31 Montage showing changes of appearance of the ion tail. Images were taken with different instruments, are not to the same scale, and only intend to show differences in the nightly appearance of the tail. All images are oriented with east towards the top and north towards the right.

Most, if not all, of the fine structure was only visible in images, and not to visual observers using binoculars or small telescopes. Nevertheless, several images give a good idea of the appearance seen in those instruments, or with the naked eye from dark sky sites. These include images by Hannetjie Minnaar on December 23 (Figure 5), Angus Burns on December 27 (Figure 15), Kos Coronaios on January 4 (Figure 25), and on January 19 (Figure 28). Gary Deacon produced an excellent sequence showing the changing appearance during the period December 21 to January 17 (Figure 32).

The images were taken with the same camera body but with different lens configurations, and consequently were resized to the same scale. They give a good idea of the changing binocular appearance as the comet passed perihelion on January 3, all the while receding from earth on the comet's return to outer space.

the house. The ion tail is complex with several streamers, brightest in p.a. 85° and 103°. Coma shows a parabolic hood, and distinctive blue colour on the sunward side [TN].



Fig. 12 December 24, 2021, Oleg Toumilovitch. Outer coma and tail are parabolic, inner coma is bright and elongated at right angles to tail direction.

Closer inspection of the inner coma in Figure 12 shows the elongated shape is maintained and shows evidence of jets feeding material into the tail [OT].

The same evening Tim Cooper imaged the coma with a 30cmT and processed the image using a Larson-Sekanina filter to give Figure 13.

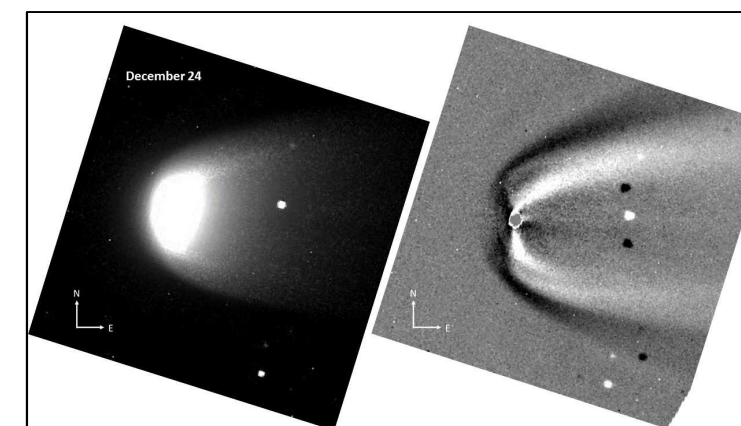


Fig. 13 December 24, 2021, Tim Cooper. Left panel is a CCD image of the comet during outburst, right panel after applying a Larson-Sekanina filter to enhance the jets emanating from the nucleus. Black dots are image artefacts introduced during the filter process. Star to the east of the coma is SAO 212679, magnitude 10.3.

This algorithm is used to improve the visibility of spiral jets emanating from the sunward side of the rotating nucleus (Larson and Sekanina 1984). The result shows evidence of prominent jets on both the north and south facing sides of the nucleus, which then sweep back towards eastwards into the tail.

December 25, 2021 – At 19h30 long tail clearly visible in 16x50B [GD].

December 26, 2021 - Figure 14 shows a clear disconnection event in the tail of the comet. The main axis of the tail is centred on p.a. $\sim 90^\circ$; the southern side has prominent filaments in p.a. 94° and 92°, and on the northern edge the tail extends to p.a. 85°. There is a knot 4.0° distant from the nucleus in p.a. 91°, the disconnection

event is at 4.6° in p.a. 90.7° . Tail length $>6^\circ$ and continues outside the field of view [JLR].

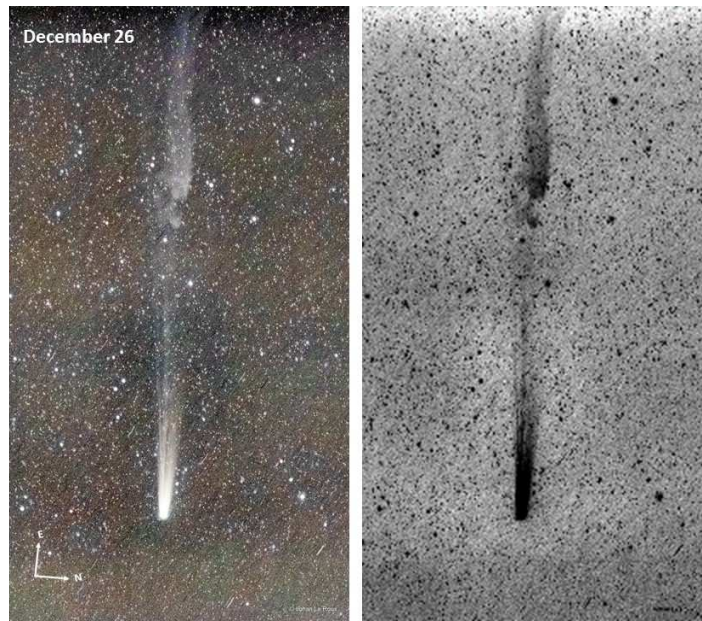


Fig. 14 December 26, 2021, Johan le Roux, showing the disconnection of the ion tail. Tail length in the image exceeds 6° and continues outside the frame at top. Bright star to the right of the head is ϵ Microscopii, magnitude 4.7.

December 27, 2021 – at 18h05, 16x50B, managed to observe briefly during a gap between two cloud bands this evening. The comet has faded to $m_1 = 4.8$, so the latest outburst is over and the comet is

returning to close to its predicted magnitude for this point in its orbit. It's still easy to find using binoculars, and displays a narrow fan-shaped tail of just over 1° length [TC]. Easy in 12x50B showing at least a 2.5° to 3° tail. With the naked eye, looks like a 3.5 to 4 magnitude star, and a tail of around 0.5° was noticeable. Seeing conditions were good with at least two observers confirming that they could see it with the naked eye [KC]. Figure 15, at last managed to observe and photograph comet this evening between clouds.



Fig. 15 December 27, 2021, Angus Burns

Tail is a narrow fan centred on p.a. 89° , length $>3^\circ$ and extends beyond the top of the enhanced image [AB]. In Figure 16, coma is elongated in the tail direction and asymmetric, bright aqua-blue on sunward side. From the coma a prominent Class R

feature at p.a. 92° extends into a bright ion tail. This splits into three separate filaments at about 0.8° from the coma. In addition a knot is visible in the middle filament, 1.7° distant from the coma in p.a. 91° [KC].

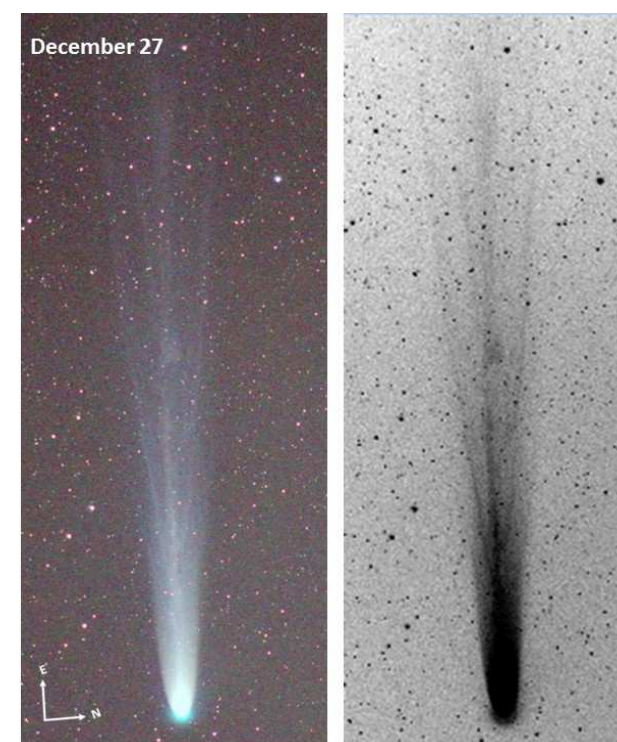
Tail development

As with the coma, observations of the tail tend to be subjective, and depend on factors intrinsic to the comet itself, but also the brightness and transparency of the sky, particularly when the moon is near its full phase, the instrument used for observation, and the presence of clouds and atmospheric pollution. When the comet first appeared from South Africa, it was low above the horizon and there was interference from twilight and bright moonlight, but with each subsequent evening the comet gained greater elevation as darkness fell and from December 20 there was a period when the comet could be observed before the moon rose in the east. Several outbursts in activity of the comet resulted in increased visibility of the tails, giving excellent opportunities for imaging and visual observation. Images by Gary Deacon taken on December 21 and Paul Ludick on December 22 showed the dust tail to be a narrow parabola, see Figures 3 and 4. The visibility of the tail increased dramatically on December 23 after the outburst in activity earlier that day, as shown in Figures 6-8 taken by Kos Coronaios, Wim Filmalter and Willie Koorts. These show a prominent ion filament in p.a. $89-90^\circ$. Twenty-four hours later the ion tail was complex, with three bright filaments and considerable fine structure as shown in Figures 10 and 11 by Lafras Smit and Tiaan Niemand. The ion tail displayed some interesting changes in appearance over the next few nights as filaments aligned with magnetic field lines in the comet's vicinity; the changing appearance is shown in Figure 31. The image by Johan le Roux on December 26 (Figure 14) shows a distinctive disconnection event, traces of which are still visible in Kos Coronaios's image twenty-four hours later (Figure 16). The turbulent nature of the interplanetary magnetic field is further evidenced by the kinks in the ion tail in Figures 17 and 18 by Tiaan Niemand and Angus Burns. A prominent Class R feature is seen in the image by Tiaan Niemand on December 28 (Figure 17), and it is also clearly seen the night after in images by Angus Burns and Lafras Smit (Figures 19 and 20). This feature is the precursor to the Type I tail proper, where ions formed under the effects of solar radiation leave the nucleus and are focused into a narrow stream by the fast-moving solar wind (Behar et al 2018).

The longest tail length measured from images was $>6^\circ$ in Figure 14 taken by Johan le Roux on December 26. However the tail in this, and many other images, extends beyond the field of view, and many concentrated on imaging the head of the comet, rather than trying to capture the full extent of the tail. Visual observations yielded much shorter tail lengths; Kos Coronaios measured the length from Pearly Beach on December 27 as 3° , while on the same evening Tim Cooper only saw a 1° tail from Bredell. Both observers used 16x50 binoculars, showing how visibility of the tail was affected by different observing conditions.

Most images show the spurious outer coma to be parabolic, see for example Figures 3, 4 and 12. Several observations indicate the inner coma was bright and irregularly shaped, particularly around the times of outbursts in activity, as Oleg Toumilovitch's images in Figure 9 show for December 22 and 23. The evening prior to outburst shows a smaller coma, elongated roughly in the anti-solar direction which is in p.a. 93° , while after outburst the coma is considerably larger and elongated in directions 25° - 205° . Observing visually on December 23, Tim Cooper reported the inner coma as bright, punctuated by a bright biconvex bar perpendicular to the tail direction. The appearance was much the same on December 24 as shown in Figures 12 and 13. The latter image by Tim Cooper shows the inner coma, which after processing with a Larson-Sekanina filter shows two prominent jets leading into the tail. By December 29 the outburst had subsided and the magnitude of the comet had returned to the normalised brightness behaviour. At the same time the coma became elongated again in the direction of the radius vector, and slightly longer along its northern side as shown by the image from Lafras Smit in Figure 20. The original image was converted to a negative, contrast enhanced and then processed to reveal contours in brightness. The shape of the coma is clearly seen in the right hand panel. This same appearance was confirmed visually, as shown in the sketch by Tim Cooper in Figure 21, but note the orientation is reversed as seen through the eyepiece.

Many images show a characteristic blue-green colour of the coma. The main contributor to the green colour in comets is fluorescence from neutral diatomic carbon (C_2) which emits light in the visible spectrum around 516.5 nm, the so-called Swan Bands. However, the colour seen in many images here (see for example Figures 2, 10-12, 17 and 20) appears to be from shorter, bluer, wavelengths. Species which contribute to colours in the blue (Feldman et al 2004) include C_3 , CH^+ (Douglas-Herzberg Bands) and CO^+ (Comet Tail Bands). However, ionized molecules would be expected to be carried into the tail under the effects of the solar wind, and therefore the distinctive colour would not be localized to the coma, especially on its sunward side. In discussions to explain the distinctive colour, Alan Fitzsimmons (2022) pointed to several possibilities. Firstly, the colour rendered by DSLR cameras depends on the filters employed and any image processing carried out, so that the colour depicted in images may not represent the true colour of the fluorescing species. Secondly the colour depends on the nature of the different C_2 emission bands, so the strongest (0-0) band around 510 nm and the (1-0) band around 550 nm will show in the green filter, but the fainter (0-1) band at 470 nm would appear in the blue filter of the image, giving the blue tinge in the combined RGB image. In addition, there is the possibility of C_3 (0-0) emission at 405 nm contributing to the blue shift in the imaged comet. Note that both the C_2 and C_3 emissions are only seen in most comets when they are within 1-2 au of the sun. They may be present at larger distances but are too faint to be detected. Both species are also rapidly photodissociated by sunlight before they reach the tail (Borsovszky et al 2021).



December 28, 2021 – At 18h16, 16x50B, $m_1 = 4.9$, coma diameter $5'$, DC = 7 [TC]. Comet and tail still visible to naked eye under good conditions, in 16x50B comet easily acquired [KC]. Figure 17, sharp bright blue coma surrounded by parabolic hood, sweeping into narrow tail. Bright spike in p.a. 94.1° , coincident with RV, leading into an ion tail which splits into three filaments in p.a. 94° at a distance of 0.3° from the coma [TN].

Fig. 16 December 27, 2021, Kos Coronaios.

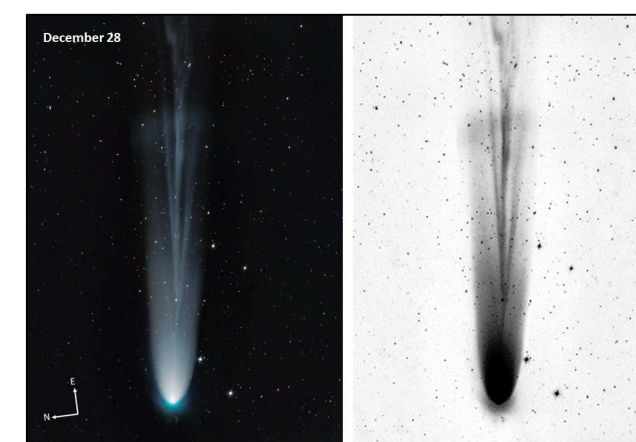


Fig. 17 December 28, 2021, Tiaan Niemand.

Figure 18, managed to image the comet between clouds, sky-glow from light pollution and haze was a real challenge, so used a Baader Neodymium filter to try and cut through it. A longer portion of tail is visible compared to Figure 17, length $>2.7^\circ$, and extends outside the field of view. The central ion filament shows several kinks [AB].

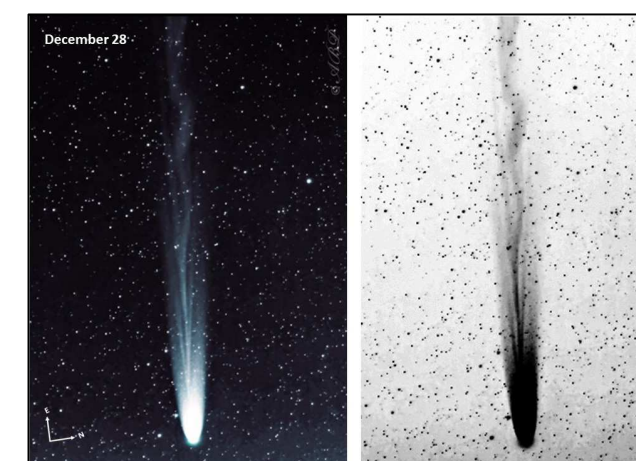


Fig. 18 December 28, 2021, Angus Burns. Note the kinks in the main ion filament.

December 29, 2021 - Figure 19, better conditions, atmosphere more stable but still quite hazy with persistent sky glow. Tail is a narrow parabola, central in p.a. 86° , length 1.9° , and width $16'$ at its widest.



Fig. 19 December 29, 2021, Angus Burns. Tail is a narrow parabola with a prominent spike leading into the ion tail.

Bright spike in p.a. 90° [AB]. Figure 20 shows the coma to be elongated and asymmetric. Sunlit side is bright aqua-blue. The bright Class R feature in p.a. 90.2° is seen to be split into two filaments [LS].

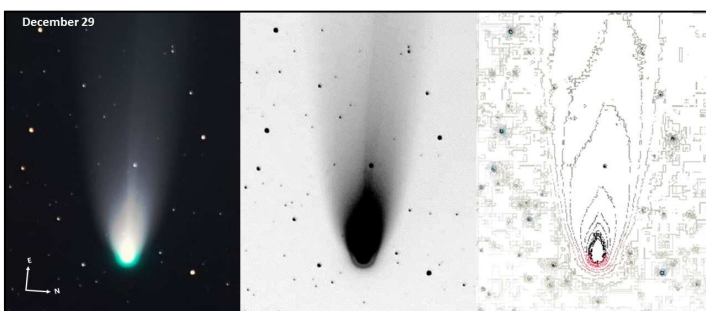


Fig. 20 December 29, 2021, Lafras Smit. Contour plot at right shows the elongated shape of the coma on its northern side.

December 30, 2021 - At 18h02, 16x50B, $m_1 = 4.8$, coma diameter = $5'$, DC = 7. Sketched at eyepiece of 30cmT, f/10, x120 between 18h05-18h24, see Figure 21.

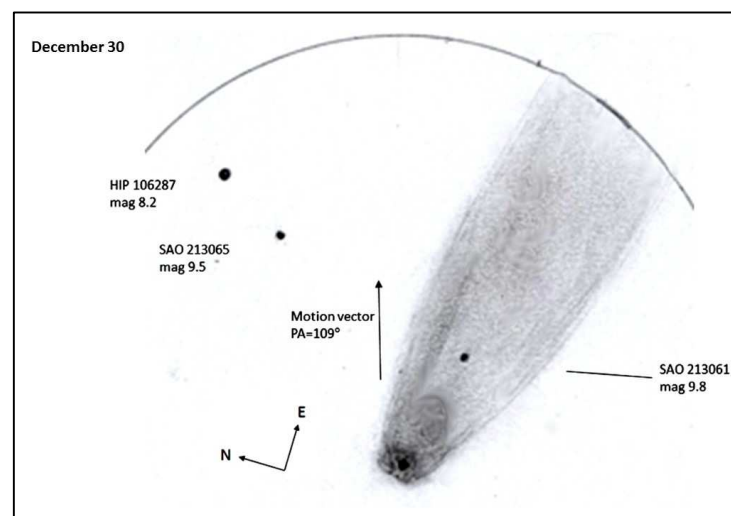


Fig. 21 December 30, 2021, sketch by Tim Cooper using 30cm Meade LX90. Note the elongated coma, and the flattened hood on the sunward side. Compare with Figure 20, but note orientation is inverted as seen through eyepiece of the SCT.

Coma is large and bright, with very bright central point, which is like a slightly defocused star, but not round, slightly elongated in the direction of the tail and surrounded by very dense inner coma. The sunward side of the coma is flattened, and appears dark, as though in shadow. The coma is elongated in the anti-solar direction and extends into the tail

Following discovery the comet increased slowly in brightness, reaching magnitude 10 during November 2021. The brightness behaviour for the period the comet was visible from southern Africa is shown in Figure 30, with the predicted brightness from Table 1 shown as a red line.

The first visual observation was by Kos Coronaios on December 18, when he estimated m_1 about 4.5, but with the comet at low altitude. On December 20, Tim Cooper found the comet an easy object despite bright twilight, and once the sky was completely dark estimated $m_1 = 3.0$ after correcting for atmospheric extinction. These observations are consistent with the light curve, and an outburst in brightness which occurred on December 20. Following this outburst, the comet became easier to locate, and more and more members of the public were also able to find the comet in binoculars once they knew where to look. After settling back down to magnitude 4, the comet underwent a further increase in brightness on December 23, increasing by half a magnitude to $m_1 = 3.5$, and now located higher above the horizon was visible to the naked eye from dark locations. Thereafter, and with the geocentric distance (Δ) of the comet now beyond 1 au, it resumed its fade, approaching the predicted brightness behaviour, and had faded to around magnitude 6 by January 11. The last observation was on January 19 by Kos Coronaios, who found the comet visible with difficulty in binoculars and in the light of a near full moon, but by then the comet had faded to near magnitude 8.

Coma morphology and colour

The Degree of Condensation (DC) of the coma was a determining factor in the visibility of the comet. In comets with low DC (1-3), the coma is spurious and often washed out from urban, light-polluted areas or under the influence of bright moonlight. In moderately condensed comets (DC 4-6) the central condensation may be visible but estimates of the brightness and coma diameter may be underestimated as the thin outer coma is also lost. As the DC increases up to DC 9, in which case the coma is observed to be star-like or a sharp disk, the comet may be more easily discerned, even under observing conditions which are less than ideal. For these reasons, and considering observing conditions vary from one observer to another, measurements of DC tend to vary considerably. However, as the comet approached the sun, actual estimates averaged DC = 4-5 (data courtesy COBS database) indicating a moderately condensed coma. During December estimates of DC = 7-8 increased, and continued through January when DC = 7 was common, indicating a strongly condensed coma. Seeing that the period of visibility for South Africa was roughly mid-December to mid-January, the strongly condensed coma and various brightness outbursts ensured good observability of the comet, and most people who had favourable weather conditions and planned carefully managed to see it.

Brightness behaviour of the comet

A few observers made visual observations or comments on the brightness of the comet. Those made according to standard ICQ procedures (Green 1997) were uploaded to the Comet Observation Database (COBS) and are included in this discussion. The complete light curve of the comet is shown in Figure 29, with the period the comet was under observation from South Africa delineated by a red box.

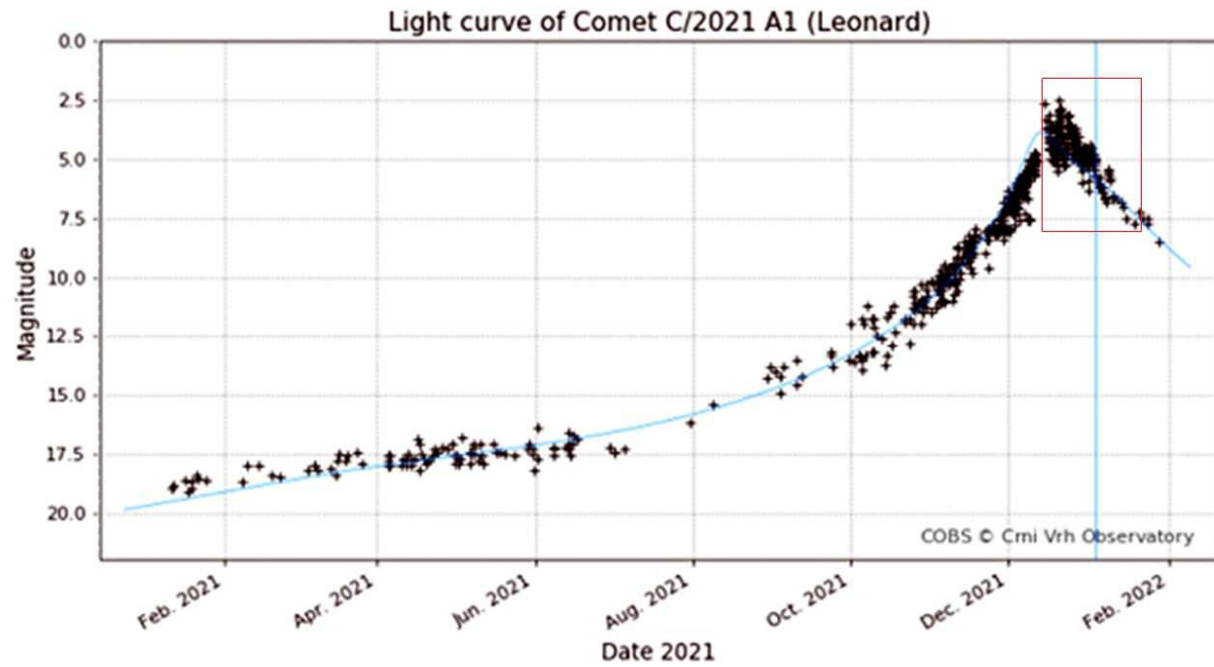
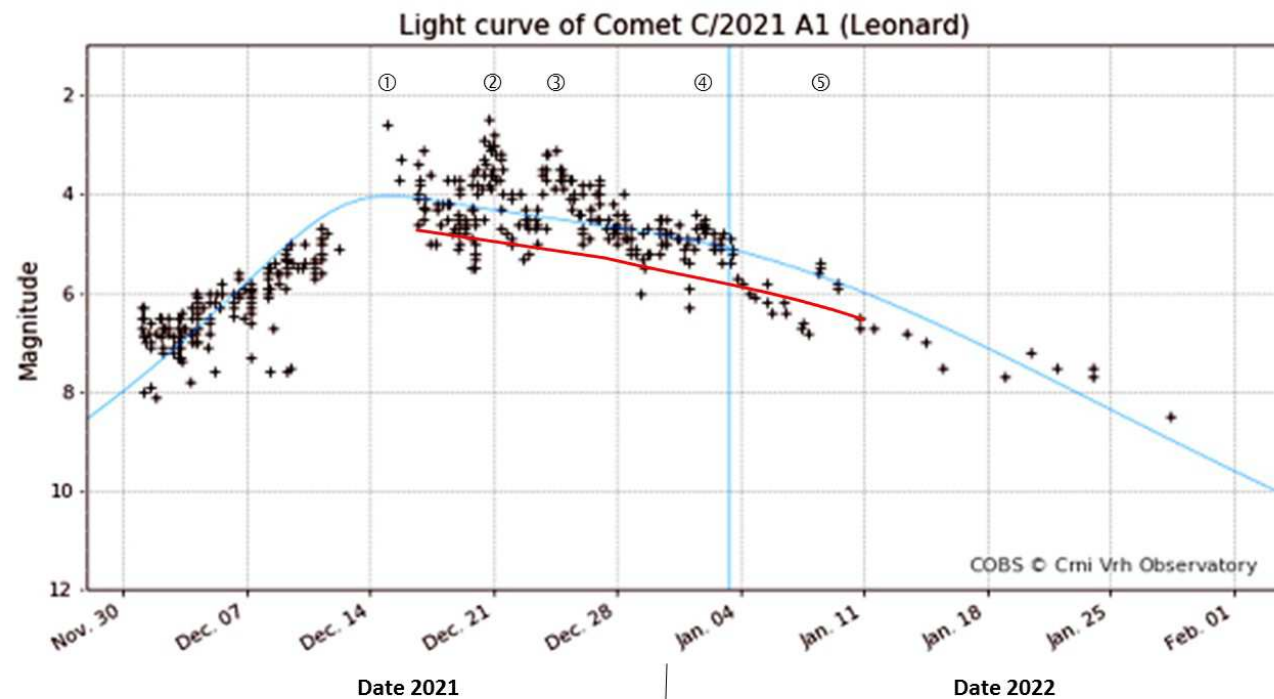


Fig. 29 light curve of the whole apparition, based on COBS data. The period the comet was under observation from South Africa is delineated by the red box.

Fig. 30 light curve of the comet including period the comet was under observation from southern Africa, and includes ASSA observations. Predicted brightness is shown as a red line, and indicates the comet became brighter than expected. 1, 2 and 3 are outbursts, 4 and 5 are also possible small enhancements in brightness.



in the direction of SAO 213061, which is in p.a. 96° , and more or less in the centre of the tail. The tail broadens into a narrow fan, is very tenuous and is accentuated in the sketch for visibility. The northern side of the tail is brighter, in about p.a. 92° [TC].

December 31, 2021 - Easily found in 12x50B, despite poor conditions, with clouds towards the west, tail at least 2.5° , difficult to detect by naked eye [KC]. Figure 22 left, several ion tail filaments visible, brightest in p.a. 91° , length $>2.2^\circ$ and continues outside the field of view [KC].

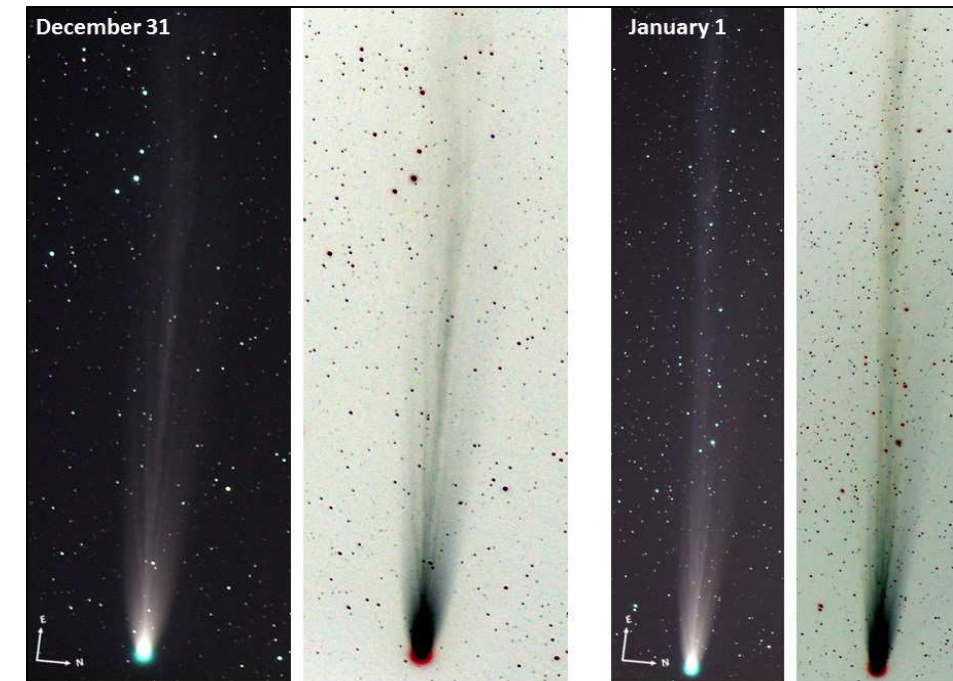


Fig. 22 December 31, 2021 left panel, and January 1, 2022 right panel, Kos Coronaios. Note changes to the ion filaments over a period of 24 hours.

Figure 23, tail is a narrow fan spanning p.a. $78-101^\circ$, ion tail brightest 1.8° in p.a. 92° [CF].

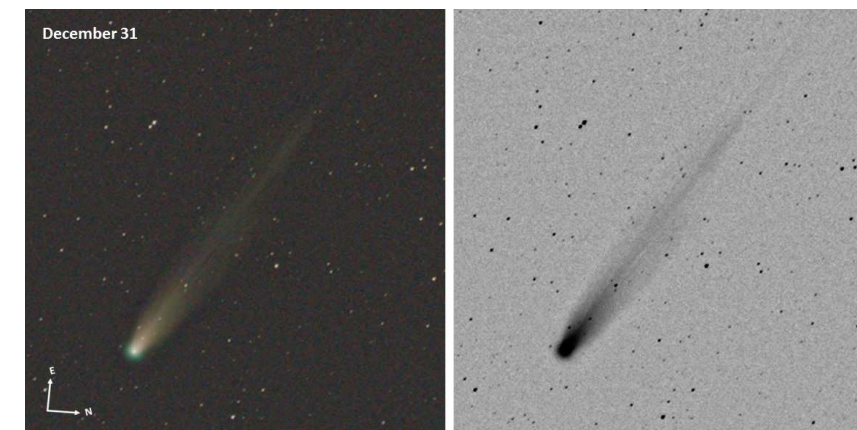


Fig. 23 December 31, 2021, Chantal Fourie.

January 1, 2022 - At 18h36, 16x50B, thin clouds and bright sky after rain, coma appears smaller and more condensed, DC = 8, but seems a little brighter than previous, $m_1 = 4.6$ [TC]. In good seeing this evening, comet was clearly seen with the naked eye including tail and was an easy binocular target in the same field of view as third magnitude γ Gruis. In 12x50B the tail could easily be seen stretching at least 3° [KC]. Using 40cmT, f/10 x100 and x240, 18h00-18h22, observed and sketched inner coma, Figure 24, coma

diameter 4.5', bright diffuse coma with hazy edge, and noticeable greenish tint on the sunward side (41mm eyepiece, x98, at 18h15).

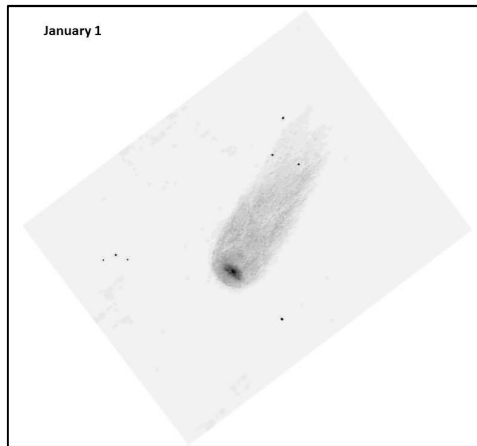


Fig. 24 January 1, 2022, sketch by Magda Streicher using 40cm Meade LX200. Note the flattened appearance of the inner coma on the sunward side. Original sketch was contrast enhanced to visualise the tenuous tail more easily.

Inner coma surrounding the nucleus is very bright and flattened on the sunward side and then fades into the tail. The nucleus is very dense like an out of focus star, magnitude 7 and about 2" diameter. The tail was barely visible, slightly fan like on the southern side and seen best with averted vision, extending out of the field of view in p.a. 98° [MS]. Figure 22 right, in comparison to the previous night, shows clear differences in the ion filaments, but brightest filament is in p.a. 95°, length >3.5° and continues outside the field of view. Despite the difference in exposure times and number of images stacked, the ion tail appears brighter and longer on January 1 than on December 31 [KC].

January 4, 2022 - One day after perihelion, still easy in 12x50B, but substantially shorter tail of around 2°, compared with previous evenings. Comet was not visible with the naked eye [KC].



Fig. 25 January 4, 2022, Kos Coronaios. The image gives a good idea of the binocular appearance of the comet from dark sky locations.

Figure 25 shows the comet in wide angle, tail is a narrow fan centred on p.a. 94°, length 2.1° [KC].



Fig. 26 January 4, 2022, Kos Coronaios.

Figure 26 image at prime focus, Class R feature in p.a. 97°, small bright coma, aqua-blue colour on sunward side, surrounded by broad parabolic envelope, extending into tail [KC].

January 8, 2022 – Figure 27, bright blue condensed coma, tail is fan-shaped but becoming indistinct. The appearance is like a shuttle-cock and spans p.a. 90-116°, brightest filament in p.a. 94°, but indistinct [OT].

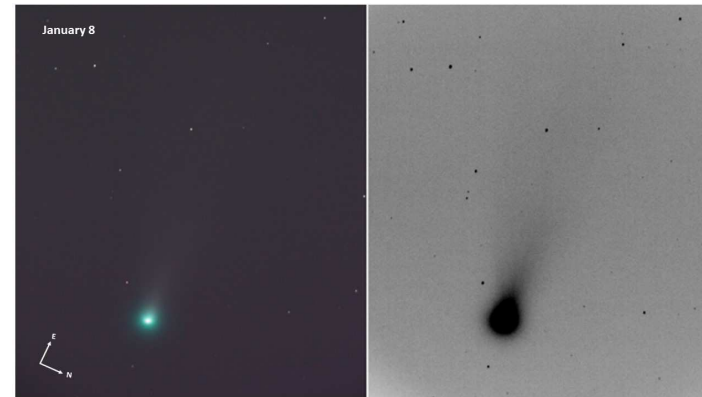


Fig. 27 January 8, 2022, Oleg Toumilovitch.

January 19, 2022 - Observed by KC, low above the horizon and with bright near-full moon, difficult in 12x50B, and not definitely visible. However, it is still impressive in 20cmT [KC].



Fig. 28 January 19, 2022, Kos Coronaios.

The last image of the comet is shown as Figure 28, tail is a narrow fan, brightest in p.a. 95° where it is traced for about 0.6°, spans p.a. 94-115° and is clearly curved towards south [KC].

January 21, 2022 - Comet is sinking fast towards the horizon now. First clear night since January 1, located position using 30cmT during bright twilight, but by the time it was dark enough to observe, the comet was below the tree line from my observatory [TC].